Modular approach for modeling a multi-energy district boiler

Julien Eynard, Stéphane Grieu, Monique Polit

Modular approach for modelling a multi-energy district boiler

Julien Eynard, Stéphane Grieu[1] and Monique Polit
ELIAUS laboratory, University of Perpignan Via Domitia, 52 Avenue Paul Alduy, 66860, Perpignan, France; {julien.eynard; grieu; polit}@univ-perp.fr

Abstract: the present paper deals with the modelling of a district boiler (city of La Rochelle, west coast of France), as part of the OptiEnR research project. This "multi-energy" boiler supplies domestic hot water and heats residential and public buildings, using mainly wood and sometimes fuel or gas if necessary. The OptiEnR research project focuses on optimizing the performance of the boiler. Its main objective is to minimize the use of fossil energy, stocking renewable energy during low-demand periods and using it when peak-demand is high. Because of both the complexity of the plant as a whole and the strong interactions between the sub-systems (the wood boiler, the gas-fuel oil boiler, the breaking pressure bottle, the cogeneration plant, the hot water distribution network), a modular approach has been proposed. According to what information is available, a combination of white, grey and black boxes (Hammerstein-Wiener models) has been used to carry out the modelling process. To answer for the lack of information, additional parameters were proposed and identified. The model has been first used in simulation during heating periods, with the aim of optimizing both the parameters of the boilers control systems and the use of wood, gas and fuel oil. Next, it will be used, when adding to the plant a thermal storage unit and implementing a Model Predictive Controller, to improve its functioning, especially reducing the coverage rate of the fossil energy boiler.

Keywords: multi-energy district boiler; hot water distribution network; modelling process; Hammerstein-Wiener model; identification; simulation; white, grey and black boxes.

Nomenclature

T_E	*Sampling time (s)*
k	*Time index (-)*
Eng_{WB}	*Wood boiler engaging (-)*
Eng_{GFB}	*Gas-fuel oil boiler engaging (-)*
$Wood_d$	*Daily consumption of wood (kg)*
$Wood_c$	*Cumulative consumption of wood (kg)*
Gas_{rt}	*Real-time consumption of gas (m³)*
Gas_d	*Daily consumption of gas (m³)*
Gas_c	*Cumulative consumption of gas (m³)*
$Fuel_{rt}$	*Real-time consumption of fuel oil (l)*
$Fuel_d$	*Daily consumption of fuel oil (l)*
$Fuel_c$	*Cumulative consumption of fuel oil (l)*
N_{tappet}	*Number of tappet strokes per five minutes (wood boiler) (-)*
T_{out}	*Outdoor temperature (°C)*
T_{SDN}	*Distribution network set-point temperature (°C)*
T_{SWB}	*Wood boiler set-point temperature (°C)*
T_{SGFB}	*Gas-fuel oil boiler set-point temperature (°C)*
T_{SC}	*Cascade set-point temperature (°C)*
T_{WB}^E	*Temperature of the water entering the wood boiler (°C)*
T_{WB}^L	*Temperature of the water leaving the wood boiler (°C)*
Q_{WB}	*Flow of the water passing through the wood boiler (m³/h)*
T_{GFB}^E	*Temperature of the water entering the gas-fuel oil boiler (°C)*
T_{GFB}^L	*Temperature of the water leaving the gas-fuel oil boiler (°C)*
T_{GFB}^{smo}	*Smokes temperature (gas-fuel oil boiler) (°C)*
Q_{GFB}	*Flow of the water passing through the gas-fuel oil boiler (m³/h)*
T_{CHC}^E	*Temperature of the water entering the collecting hydraulic circuit (°C)*
T_{CHC}^L	*Temperature of the water leaving the collecting hydraulic circuit (°C)*
Q_{CHC}	*Flow of the water passing through the collecting hydraulic circuit (m³/h)*
T_{DB}	*District boiler ambient temperature (°C)*
T_{CGP}^E	*Temperature of the water entering the cogeneration plant (°C)*
T_{CGP}^L	*Temperature of the water leaving the cogeneration plant (°C)*
Q_{CGP}	*Flow of the water warmed up by the cogeneration plant (m³/h)*

[1]*Corresponding author. Tel.: +33 468662202; fax: +33 468662287.*

W_{CGP}	*Power provided by the cogeneration plant (W)*
E_{CGP}	*Energy provided by the cogeneration plant (Wh)*
T_{DN}^{E}	*Temperature of the water entering the distribution network (°C)*
T_{DN}^{L}	*Temperature of the water leaving the distribution network (°C)*
Q_{DN}^{E}	*Flow of the water entering the distribution network (m³/h)*
T_{BPB}^{E}	*Temperature of the water entering the breaking pressure bottle (°C)*
T_{BPB}^{L}	*Temperature of the water leaving the breaking pressure bottle (°C)*
Q_{BPB}^{L}	*Flow of the water leaving the breaking pressure bottle (m³/h)*
P_{DN}	*Water differential pressure (distribution network) (bar)*
P_{SDN}	*Water differential pressure set-point (distribution network) (bar)*
Q_{BPB}^{H}	*Horizontal flow inside the breaking pressure bottle (m³/h)*
Q_{BPB}^{up}	*Vertical flow inside the breaking pressure bottle (updraft flow) (m³/h)*
Q_{BPB}^{down}	*Vertical flow inside the breaking pressure bottle (downdraft flow) (m³/h)*
$\%_{fp}$	*Opening percentage of the valve of the distribution network feed pump (%)*
W_{DN}	*Thermal power consumed by the distribution network (W)*
Q_{prod}	*Production flow (m³/h)*
W_{prod}	*Production power (W)*
E_{prod}	*Production energy (Wh)*
T_{prod}^{up}	*Temperature of the water passing through the internal circuit of the cogeneration plant, before being cooled down by the "cogeneration/network" exchanger (°C)*
T_{prod}^{down}	*Temperature of the water passing through the internal circuit of the cogeneration plant, after being cooled down by the "cogeneration/network" exchanger (°C)*
$\%_{fh}$	*Opening percentage of the valve of the fan-heater unit (%)*
W_{fh}	*Fan-heater power dissipation (W)*
T_{PR}^{L}	*Temperature of the water cooled down by the pressure regulator (°C)*
T_{ECE}^{L}	*Temperature of the water warmed up by the "engine/cogeneration" exchanger (°C)*

1. Introduction

Managing energy demand, promoting renewable energy and finding ways to save energy are worldwide concerns as well as innovative solutions to fight the global energy crisis (mainly caused by both the rarefaction of fossil fuels and an excessive energy consumption: many experts believe that by 2015 the supply of oil and natural gas will be unable to keep up with demand [1]). Renewable energy is one of the ways to limit both GreenHouse Gases (GHG) emissions and the impact of climate change on environment and health. That is why the European Council's ambitious objectives of saving 20% of the energy consumption compared to projections for 2020, of reducing of at least 20% the GHG emissions compared to the 1990 level and, finally, of raising the share of renewable energy sources in its final energy consumption from around 8.5% in 2005 to 20% in 2020 then to 50% in 2040 plays a central role in the EU energy policy [2].

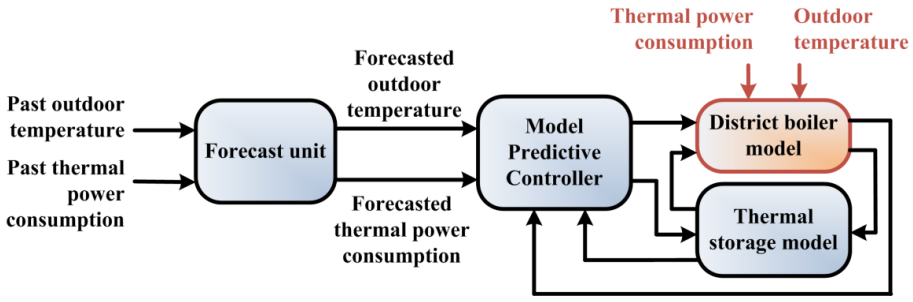

Figure 1. The OptiEnR project. In red, the district boiler model presented in the paper.

As part of the OptiEnR research project, the present paper, the second of a series of three [3] dealing with the optimization of the performance of a district boiler, focuses on its analysis and modelling. The just-mentioned project began in late 2008 and finished in late 2010. It involves researchers from the ELIAUS laboratory of the University of Perpignan Via Domitia (south of France) and engineers from two French companies, Cofely GDF-SUEZ [4] and Weiss France [5]. Cofely GDF-SUEZ is currently the leading European brand for environmental and energy efficiency services while Weiss France designs, manufactures and installs automatic boiler rooms

for all types of wood, biomass, wastes and fluids. The district boiler will be described later in the present paper (section 2) and is situated at La Rochelle (west coast of France). It is managed by Cofely GDF-SUEZ, supplies domestic hot water and heats residential and public buildings, using mainly wood and sometimes fuel or gas if necessary. The OptiEnR project focuses on improving the performance of the plant (first optimizing the parameters of the boilers control systems), using a model-based predictive controller to manage a to-be-implemented thermal storage unit (while adding new pumps). Its main objective is to minimize the use of fossil energy, stocking renewable energy during low-demand periods and using it when peak-demand is high. The project consists of the following successive tasks (Figure 1): the first task is to forecast outdoor temperature and thermal power consumption (of the hot water distribution network) [3]; the second task focuses on modeling the district boiler; the third task deals with studying the feasibility of adding to the plant a thermal storage unit and finding the most adequate storage material; the fourth task is to model the thermal storage while the fifth task focuses on optimizing the boiler functioning using both a Model Predictive Controller (MPC) [6-7] and the forecasted parameters (first task). The present paper deals with the second task, the next paper of the series dealing with the tasks 3 to 5.

Taking a look at the state of the art about the modelling of district boilers, one can highlight some interesting works. First, Curti *et al.* proposed in 2000 [8] an "environomic" approach for modelling and optimizing a district heating network based on both centralized and decentralized heat pumps, cogeneration and/or gas furnace. Because adapting the delivery temperature to the most exigent users is detrimental to the overall system performance, the authors proposed to centralize its management. Its environmental characteristics are introduced into the proposed model through pollution damage cost terms and a new form of pollution penalty functions, which adapt to the system's changing emissions and to local and global pollutant conditions. Although a centralized management can be effective, such an orientation is questionable in case of multi-component systems or when the behaviour of some components and/or the internal organisation of the plant (and, as a consequence, the way these elements impact each other) is not easy to understand. Next, Dias *et al.* [9] modelled a wood boiler via a detailed energy and exergy analysis. Inefficiencies in a process are well pinpointed when carrying out this kind of study because an exergy analysis allows quantifying the types, causes, and locations of losses. Such an approach can be considered to model all the type of gas and wood boilers, used to produce hot water. However, it can be hard to conduct in case of very complex systems (such as multi-energy systems dealing with several energy resources) or when information is (partially) missing or corrupted. Although exergy analysis is a very efficient tool for process optimization and understanding, performing such an analysis at the district boiler of La Rochelle was not possible. Gonzalez-Bustamante *et al.* [10] proposed a method to model the transients in a natural gas line which supplies a boiler at a stream-electric power plant. The proposed solution permits to both carrying out a dynamic analysis of the boiler and designing regulation and control tools at a reasonable cost for industrial projects. However and because of its specificity, this method can be hardly applied to others boilers. Niu *et al.* [11], Prasad [12] and Mahlia *et al.* [13] works focused on modelling boilers used to produce electricity. Niu *et al.* [11] highlighted that industrial boilers will behave differently due to manufacturing or assembly tolerance. In addition, the performance of a boiler will vary at different times of its service life. That why their paper deals with both the modelling and the simulation of a boiler unit to highlight such an issue. In the boiler model, heat transfer in the combustion chamber is simulated by the zone method while heat transfer in the primary and the secondary superheaters, in the reheater and in the economizer is simulated by lump parameter analysis. The main feature of the method used is that the respective models of the major components have been coupled sequentially according to the boiler configuration. Thus, the authors assume that the method they proposed may be applied to different boiler systems with different configurations. However, one can highlight that a thorough understanding of the various phenomena involved is absolutely necessary. Finally, the uncertainly factors, such as, for examples, water tube deposits or components deterioration, are considered by modification factors which are determined from on-line measurements. Prasad's paper [12] deals with the theoretical performance of a biomass-fuelled boiler/steam power cogeneration system. He based the system performance on the known and assumed properties of the biomass fuel (its size, elemental composition or moisture content), on energy content of the combustible constituents (fuel) and on load profiles. As a consequence, this approach can be hard to implement if the just-mentioned properties are not well defined or when they vary in time. Mahlia *et al.* [13] developed a state-space dynamic model for a palm wastes boiler. The unique feature of the boiler is that it uses

wastes in the form of fiber and shell from the palm oil processing as its fuels. Specific characteristics of oil palm waste boilers are non-uniform fuel feed, compositions, sizes and moisture content of the fuel. The boiler unit has been divided into several sub-systems. The linearized model consisted of ten first-order simultaneous equations. All of these works [8-13] are really interesting but do not match with the constraints imposed by the multi-energy district boiler of La Rochelle (where information is partially missing), its proper characteristics (for example, the cogeneration plant produces electricity and warms a part of the cold water coming back from the distribution network) and the goal set by Cofely GDF-SUEZ. Of course, efficiently modelling a boiler requires expert knowledge about physical parameters. When information is partially missing, one can use alternative and well-known methods, such as bond graphs, fuzzy logic, artificial neural networks or genetic algorithms. Bouamama *et al.* [14] used bond graphs to model a steam generator installation consisting of various complex industrial components, such as a boiler or a condenser. As shown by the authors in their paper, bond graph modelling is a suitable tool to represent the model structures of such processes along with their control system instrumentation. A structural analysis of the model allowed the authors to determine the fault signatures. Hardware redundancies in the sensor placement have also been highlighted. Finally, a supervision platform including reconfiguration strategies has been proposed. However, and because bond graphs are designed around the conservation principles of physics, they are only suitable for the description of physical systems. Chemistry is a border-line case. For the present study, the complexity of the district boiler of La Rochelle makes hard to use this tool. Lu *et al.* [15] developed a nonlinear power plant (a 200 MW oil-fired drum-type boiler-turbine-generator unit) model, taking into account physical principles and using artificial neural networks. Practical aspects of neural network modelling were investigated to ensure sufficient perturbations covering proper dynamic and load conditions. The simulation results showed that the accuracy of artificial neural network models depends greatly on the training data and is satisfactory within normal operating scope. Artificial neural networks were also used by Romeo and Gareta [16] for monitoring a biomass boiler. The authors highlight that biomass combustion produces fouling in boiler heat transfer equipment causing a reduction of steam output and boiler efficiency. That is why artificial neural networks were used to predict a set of operational variables and the fouling state of the boiler. However, more research is required for minimize the fouling effect once it has been detected. As one knows, multilayer feedforward neural networks are a class of universal and parsimonious approximators. Such networks can be used to model and/or control complex and nonlinear systems. However, their generalization capability is strongly related to the relevance of the training examples used. That is why, due to the limited quantity of historical data available at the district boiler of La Rochelle, such an approach has not been considered. Finally, Ghaffari *et al.* [17] presented a soft computing approach for modelling electrical power generating plants with the aim of characterizing the essential dynamic behaviour of the plant sub-systems. The proposed approach consisted of fuzzy logic, artificial neural networks and genetic algorithms. The data measured from a complete set of field experiments is the basis for training the models, including the extraction of linguistic rules and membership functions as well as adjusting the other parameters of the fuzzy model. The genetic algorithm has been used to optimize the training procedures.

According to all the just-mentioned considerations and because of both the complexity of the district boiler of La Rochelle as a whole and the strong interactions between the sub-systems (the wood boiler, the gas-fuel oil boiler, the breaking pressure bottle, the cogeneration plant…), a modular approach has been proposed for modelling the plant. According to what information is available (provided by measurement campaigns or taking into consideration expert knowledge about the sub-systems functioning and the boilers control systems), a combination of white, grey and black boxes has been used. With white boxes, which are used when one can easily describe the interactions between physical parameters, experimental data are only used to validate the developed models. Both grey boxes [18] (in this case one needs to find appropriate model inputs and outputs, thanks to some physical considerations and/or analyzing the process dynamic properties; experimental data allow, first, optimizing both the model topology and parameters [19-20] and, secondly, validating this model) and black boxes (with this kind of models, no physical considerations are taken into account; a standard topology is used and, as when using grey boxes, one needs to find appropriate model inputs and outputs and to optimize, thanks to experimental data, the model parameters) [18] are used in case of missing information about physical behaviour. Let us note that in some cases, additional parameters were proposed and identified to answer for the lack of information. The developed model has been first used in simulation during heating

periods, with the aim of optimizing both the parameters of the boilers control systems and the use of wood, gas and fuel. As previously mentioned, the model will be used, when adding to the plant a thermal storage unit and implementing a predictive optimal controller, to optimize its functioning, especially reducing the coverage rate of the fossil energy boiler.

2. The district boiler of La Rochelle

The district boiler of La Rochelle, whose synopsis is shown in Figure 2, is composed of a breaking pressure bottle, a cogeneration plant and two thermal boilers. The first one, a large 4.5 MW wood boiler, uses renewable energy (it is fed with woodchip). The second one, a 7 MW gas-fuel oil boiler, uses fossil energy. Both boilers have smokes and air-to-water heat exchangers. They supply hot water to the collecting hydraulic circuit according to a temperature set-point which is defined from outdoor temperature. During the cold season (from October to May), the wood boiler is continuously running while its heating power is adapted to the demand. The gas-fuel oil boiler functions during very cold periods only, when the wood boiler fails to respond to the demand. The primary hydraulic circuit (3000 m^3), or "distribution network", supplies hot water to heat residential and public buildings (for example schools), for a total of 2700 accommodations. Domestic hot water is also produced, for a total of 3500 accommodations. The cogeneration plant, connected to the "return" part of the primary hydraulic circuit, produces electricity using gas and warms up the cold water before it goes back to the collecting hydraulic circuit. The breaking pressure bottle pulls apart the two hydraulic circuits, because of the difference between their respective flows.

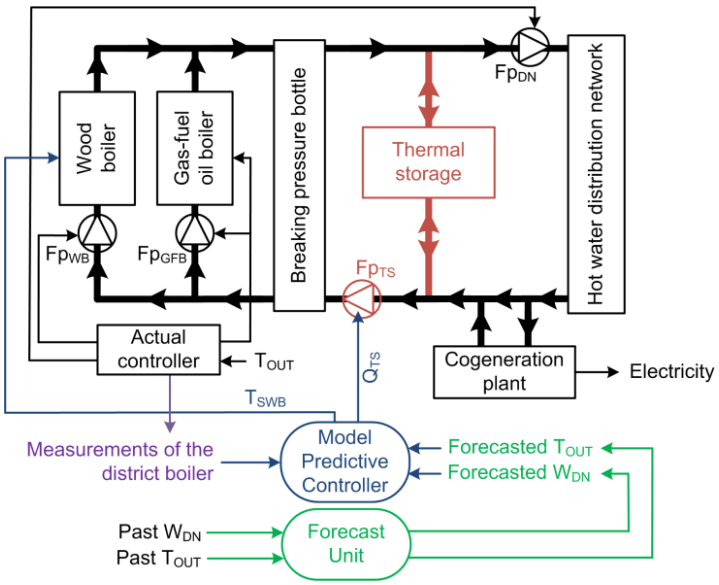

Figure 2. Synopsis of the district boiler of La Rochelle. In black, the main components of the plant and in red, blue and green, the modifications proposed to improve its performance.

The coverage rates of the three heat generators are 50% (wood boiler), 15 to 20% (gas-fuel oil boiler) and 30 to 35% (cogeneration plant), respectively. To minimize the gas-fuel oil boiler coverage rate, we proposed to add a thermal storage unit to the plant (Figure 2) with the aim of stocking hot water when the demand is low and using it when the demand can't be met by the wood boiler. This is a classical solution to optimize the functioning of boilers used to heat buildings [21-23]. Thus, the gas-fuel oil boiler will be only used when both the hot water demand is very high and the thermal storage unit is empty. The flow of the water passing through this unit (Q_{TS}) will be adjusted thanks to the control of the thermal storage feed pump (Fp_{TS}). With the aim of optimizing the use of this thermal storage unit and reducing the fossil boiler coverage rate, a model predictive controller will define over the next 4 hours and 30 minutes the optimal sequence of Q_{TS} and the wood boiler set-point temperature (T_{SWB}), taking into consideration some parameters measured at the district boiler as well as both the forecasted outdoor temperature (T_{out}) and thermal power consumption (of the distribution network) (W_{DN}). The wood boiler (Fp_{WB}) and gas-fuel oil boiler (Fp_{GFB}) feed pumps are controlled using a standard on/off controller. Fp_{DN} is the distribution network feed pump (Figure 2).

3. Experimental data

For most of the experimental parameters used to model the multi-energy district boiler of La Rochelle, T_E is equal to 300 seconds (5 minutes). For some parameters measured every 15 minutes or every hour only, data were interpolated (i.e. upsampled) to be in agreement with the just mentioned sampling time. Measurement campaigns were carried out during the winter period of 2009, from early January to late March. During this period, the district boiler behaviour is fully representative of a typical behaviour for such a plant.

4. Modelling of the district boiler

4.1. Proposed approach

As previously mentioned, because of both the complexity of the district boiler of La Rochelle as a whole and the strong interactions between sub-systems, a modular approach is proposed for modelling the plant. First, a data processing phase allowed eliminating abnormal (acquired) data and upsampling data with a too-high sampling rate. Let us also note that some relevant but not-measured parameters have been estimated thanks to appropriate information. Next, for each parameter to be modelled, both the model topology (a differential, algebraic or logical equation) and the model inputs are defined. An iterative process of optimisation has been performed to identify the coefficients of the models. We used the trust-region reflective Newton method for nonlinear least-squares to solve the minimization problem [24-26]. Analysing the results allows validating the chosen topologies (if a result is not satisfactory, one needs to think about another model topology and to find the right equation coefficients again). With the boiler parameters correctly described, using optimized differential, algebraic of logical equations, sub-models (about sub-systems such as the wood boiler, the gas-fuel oil boiler, the breaking pressure bottle, the cogeneration plant…), which inputs are only exogenous ones, are defined. A second iterative process of optimisation is carried out to adjust the sub-models coefficients. Finally, when the sub-models accuracy is as good as possible, these models are combined to obtain the district boiler model.

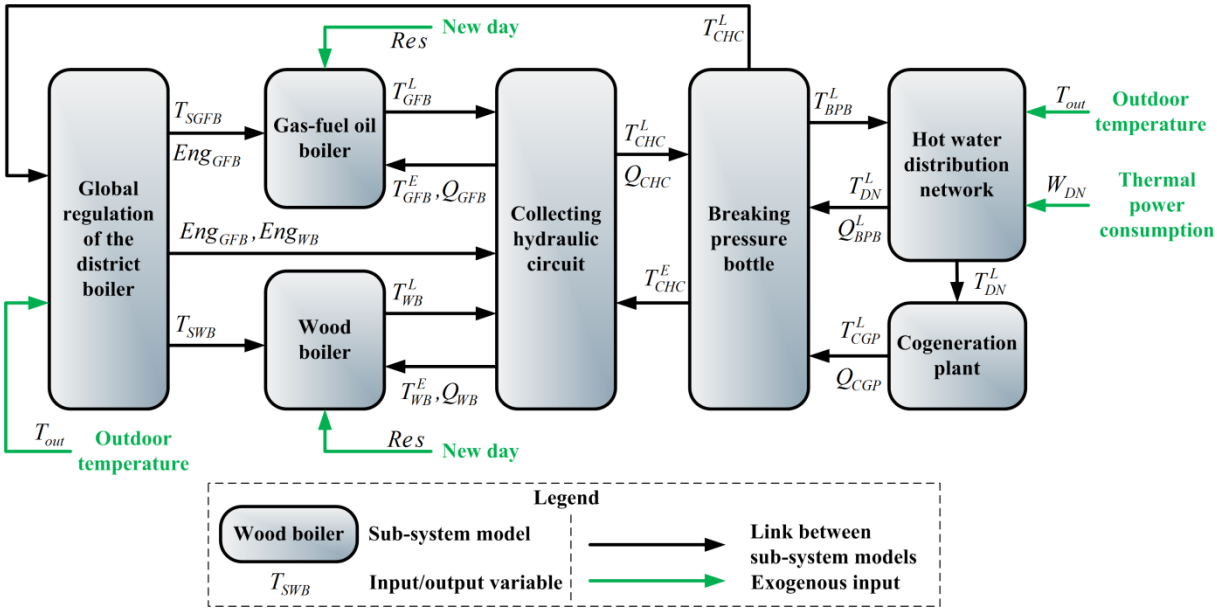

Figure 3. Modular approach for modelling the district boiler of La Rochelle.

Figure 3 depicts the way the district boiler of La Rochelle is modelled, via a modular approach based on interconnected sub-models. Only two exogenous model inputs are considered: the outdoor temperature and the thermal power consumption of the distribution network. These inputs are forecasted over the next 4h30, as requested by the boiler operators and taking into consideration the main objective of the OptiEnR project. The forecasting methodology deals with the concept of time series and uses a wavelet-based multi-resolution analysis and Artificial Neural Networks (ANN) [3, 27-29]. Substituting the prediction task of an original time series of high variability by

the prediction, using ANN, of its wavelet coefficients on different levels of lower variability (according to different frequency domains) was the main idea when developing this methodology. Then, the reconstruction of the target sequences was performed by simply summing up these coefficients. With simulations, one can understand the way the outdoor temperature and the thermal power consumption of the distribution network impact on the district boiler behaviour.

4.2. Global regulation of the district boiler

The distribution network (T_{SDN}), the wood boiler (T_{SWB}) and the gas-fuel oil boiler (T_{SGFB}) set-point temperatures, the cascade set-point temperature (T_{SC}) as well as the way the two boilers are engaged or stopped (Eng_{WB} and Eng_{GFB}) are specified according to both the outdoor temperature (T_{out}) and the temperature of the water leaving the collecting hydraulic circuit (T_{CHC}^{L}) (section 4.5.3). The network set-point temperature is the temperature we want for the water in the primary hydraulic circuit.

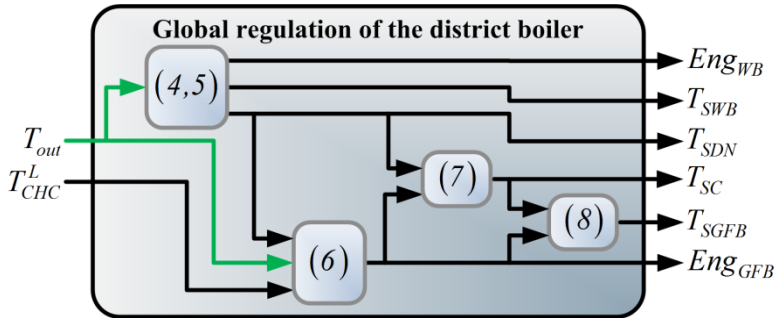

Figure 4. Global regulation of the district boiler (in brackets, the model equations).

4.2.1. Distribution network set-point temperature

The distribution network set-point temperature is calculated using a piecewise affine linear function of outdoor temperature. This function is composed of four linear pieces, defined according to the following coordinates $\{(T_{out\_SDN_1}; T_{SDN_1}), (T_{out\_SDN_2}; T_{SDN_2}), \dots, (T_{out\_SDN_5}; T_{SDN_5})\}$, which respective parameters need to be identified. As a result, one can model the way the network set-point temperature is evolving, using conditional (algebraic) equations (1). $\forall i \in [1,4]$, $a_{SDN_{i,i+1}}$ and $b_{SDN_{i,i+1}}$ are defined by equations (2) and (3), respectively:

$$\begin{cases} if\ T_{out} < T_{out\_SDN_1}\ then\ T_{SDN} = T_{SDN_1} \\ if\ T_{out\_SDN_1} \le T_{out} \le T_{out\_SDN_2}\ then\ T_{SDN} = a_{SDN_{1,2}} \cdot T_{out} + b_{SDN_{1,2}} \\ if\ T_{out\_SDN_2} \le T_{out} \le T_{out\_SDN_3}\ then\ T_{SDN} = a_{SDN_{2,3}} \cdot T_{out} + b_{SDN_{2,3}} \\ if\ T_{out\_SDN_3} \le T_{out} \le T_{out\_SDN_4}\ then\ T_{SDN} = a_{SDN_{3,4}} \cdot T_{out} + b_{SDN_{3,4}} \\ if\ T_{out\_SDN_4} \le T_{out} \le T_{out\_SDN_5}\ then\ T_{SDN} = a_{SDN_{4,5}} \cdot T_{out} + b_{SDN_{4,5}} \\ if\ T_{out} > T_{out\_SDN_5}\ then\ T_{SDN} = T_{SDN_5} \end{cases} \quad (1)$$

$$a_{SDN_{i,i+1}} = \frac{T_{SDN_{i+1}} - T_{SDN_i}}{T_{out\_SDN_{i+1}} - T_{out\_SDN_i}} \quad (2)$$

$$b_{SDN_{i,i+1}} = T_{SDN_i} - a_{SDN_{i,i+1}} \cdot T_{out\_SDN_i} \quad (3)$$

One can reformulate the just-mentioned equation system (1) (both $a_{SDN_{i,i+1}}$ and $b_{SDN_{i,i+1}}$ remain unchanged) using logical (algebraic) equations, $\forall i \in [1,4]$ and $\forall j \in \{0;5\}$, in the following way (4):

$$\begin{cases} \delta_{SDN_{0,1}} = T_{out} \le T_{out\_SDN_1} \\ \delta_{SDN_{i,i+1}} = (T_{out\_SDN_i} \le T_{out}) \wedge (T_{out} \le T_{out\_SDN_{i+1}}) \\ \delta_{SDN_{5,6}} = T_{out} \ge T_{out\_SDN_5} \\ a_{SDN_{j,j+1}} = 1\ and\ b_{SDN_{j,j+1}} = 0 \\ T_{SDN} = \sum_{m=0}^{5} \left(\delta_{SDN_{m,m+1}} \cdot \left(a_{SDN_{m,m+1}} \cdot T_{out} + b_{SDN_{m,m+1}} \right) \right) \end{cases} \quad (4)$$

4.2.2. Wood boiler set-point temperature

The wood boiler set-point temperature is the temperature we want for the water leaving this boiler. As for the network set-point temperature, it is calculated using a piecewise affine linear function of outdoor temperature. Again, the function coefficients need to be identified. As a result, one can model the way the wood boiler set-point temperature is evolving, using the following logical (algebraic) equations (5), $\forall i \in [1,3]$ and $\forall j \in \{0;4\}$:

$$\begin{cases} \delta_{SWB_{0,1}} = T_{out} \leq T_{out\_SWB_1} \\ \delta_{SWB_{i,i+1}} = \left(T_{out\_SWB_i} \leq T_{out}\right) \wedge \left(T_{out} \leq T_{out\_SWB_{i+1}}\right) \\ \delta_{SWB_{4,5}} = T_{out} \geq T_{out\_SWB_4} \\ a_{SWB_{j,j+1}} = 1 \text{ and } b_{SWB_{j,j+1}} = 0 \\ a_{SWB_{i,i+1}} = \frac{T_{SWB_{i+1}} - T_{SWB_i}}{T_{out\_SWB_{i+1}} - T_{out\_SWB_i}} \\ b_{SWB_{i,i+1}} = T_{SWB_i} - a_{SWB_{i,i+1}} \cdot T_{out\_SWB_i} \\ T_{SWB} = \sum_{m=0}^{4} \left(\delta_{SWB_{m,m+1}} \cdot \left(a_{SWB_{m,m+1}} \cdot T_{out} + b_{SWB_{m,m+1}}\right)\right) \end{cases} \quad (5)$$

Let us remember that we describe the way the wood boiler functions thanks to Eng_{WB}. This is a binary variable. We suppose the wood boiler to be continuously functioning. It stops only in case of failure but we do not consider such an event ($Eng_{WB} = 0$). As a consequence, $Eng_{WB} = 1$.

4.2.3. Gas-fuel oil boiler engaging

The working of the gas-fuel oil boiler is relatively complex. First, this boiler only works when outdoor temperature is below 0°C. If so, shutdown and restart sequences depend on the difference between T_{SDN} and T_{CHC}^{L}. If this difference is greater than 3°C (ε_1), with $T_{CHC}^{L} < T_{SDN}$, during a continuous and minimal period of time (t_{GFB}^{Eng}) of 10 min, the gas-fuel oil boiler starts working. It works until $T_{CHC}^{L} - T_{SDN} > 1$°C ($\varepsilon_2$), with $T_{CHC}^{L} > T_{SDN}$. Let us note that the boiler can only stop working if it was in service during the last 2 hours and 10 minutes (t_{GFB}^{Sto}). These values were provided by Cofely GDF-SUEZ. The way the gas-fuel oil boiler functions is described by the following equation system (6), with $C_1^{Eng_{GFB}}$, $C_2^{Eng_{GFB}}$, $C_3^{Eng_{GFB}}$ and $C_4^{Eng_{GFB}}$ reporting if outdoor temperature is below 0°C, if just before the gas-fuel oil boiler stops, the outdoor temperature was higher than 0°C, if $T_{SDN} - T_{CHC}^{L}$ is greater than 3°C and if, due to outdoor temperature, the gas-fuel oil boiler has to stop working, respectively. $Del_{GFB}^{Eng} = 60$ seconds and $Del_{GFB}^{Sto} = 130$ min are the engaging and stopping delays. k is the time index while T_E is the sampling time:

$$\begin{cases} C_1^{Eng_{GFB}} = T_{out}(k) \leq 0 \\ C_2^{Eng_{GFB}} = \left(1 - Eng_{GFB}(k)\right) \wedge \left(1 - C_1^{Eng_{GFB}}\right) \\ C_3^{Eng_{GFB}} = C_2^{Eng_{GFB}} \wedge \left((T_{SDN} - T_{CHC}^{L}) > \varepsilon_1\right) \\ C_4^{Eng_{GFB}} = Eng_{GFB}(k) \wedge \left(1 - C_1^{Eng_{GFB}}\right) \\ Del_{GFB}^{Eng}(k+1) = \left(C_1^{Eng_{GFB}} + C_4^{Eng_{GFB}}\right) \times \left(Del_{GFB}^{Eng}(k) + T_E\right) \\ Del_{GFB}^{Sto}(k+1) = C_3^{Eng_{GFB}} \times \left(Del_{GFB}^{Sto}(k) + T_E\right) \\ C_5^{Eng_{GFB}} = C_2^{Eng_{GFB}} \wedge \left(Del_{GFB}^{Eng}(k+1) \geq t_{GFB}^{Eng}\right) \\ C_6^{Eng_{GFB}} = C_4^{Eng_{GFB}} \wedge \overline{\left(\left((T_{CHC}^{L} - T_{SDN}) > \varepsilon_2\right) \wedge \left(Del_{GFB}^{Sto}(k+1) > t_{GFB}^{Sto}\right)\right)} \\ Eng_{GFB}(k+1) = C_1^{Eng_{GFB}} + C_5^{Eng_{GFB}} + C_6^{Eng_{GFB}} \end{cases} \quad (6)$$

Let us note, first, that Eng_{GFB} will be used to correctly formulate the gas-fuel oil boiler set-point temperature (section 4.2.4) and, secondly, that Del_{GFB}^{Eng} and Del_{GFB}^{Sto} were optimised to satisfy experimental data.

4.2.4. Gas-fuel oil boiler set-point temperature

The gas-fuel oil boiler only works when the global regulator orders, with the aim of being in agreement with the distribution network set-point temperature. That is why we want T_{SGFB} to be

equal to zero when the gas-fuel oil boiler does not work and equal to the network set-point temperature when it does. First we use Eng_{WB} to define the cascade set-point temperature (T_{SC}) as follows (7):

$$T_{SC} = Eng_{GFB} \cdot T_{SDN} \tag{7}$$

With the aim of avoiding a too-abrupt start-up of the gas-fuel oil boiler, caused by a set-point temperature higher than the initial temperature of the water inside the boiler, T_{SC} is filtered. However, when the gas-fuel oil boiler has to be stopped, it has to be done immediately to limit the consumption of fossil energy. For that purpose, Eng_{GFB} will be used. According to the just-mentioned considerations, T_{SGFB} is defined in the following way, with $\alpha^{T_{SGFB}}$ and $\beta^{T_{SGFB}}$ two coefficients to be identified and k the time index (8):

$$T_{SGFB}(k+1) = Eng_{GFB} \cdot (\alpha^{T_{SGFB}} \cdot T_{SGFB}(k) + \beta^{T_{SGFB}} \cdot T_{SC}(k)) \tag{8}$$

4.2.5. Identification results

Table 1 (Appendix) summarizes the results of the identification process. Over-all, these results can be considered as satisfactory, in particular for both the distribution network (T_{SDN}) (Figure 4) and the wood boiler (T_{SWB}) (Figure 5) set-point temperatures which are only calculated using outdoor temperature. Experimental ($Data_{exp}$) and simulated ($Data_{sim}$) data are compared calculating the Mean Relative Error (MRE) and the curve fitting (FIT), a widely-used similarity criterion (9):

$$FIT = 100 \times \left(1 - \frac{\left\| Data_{sim} - Data_{exp} \right\|_2}{\left\| Data_{exp} - \langle Data_{exp} \rangle \right\|_2}\right) \tag{9}$$

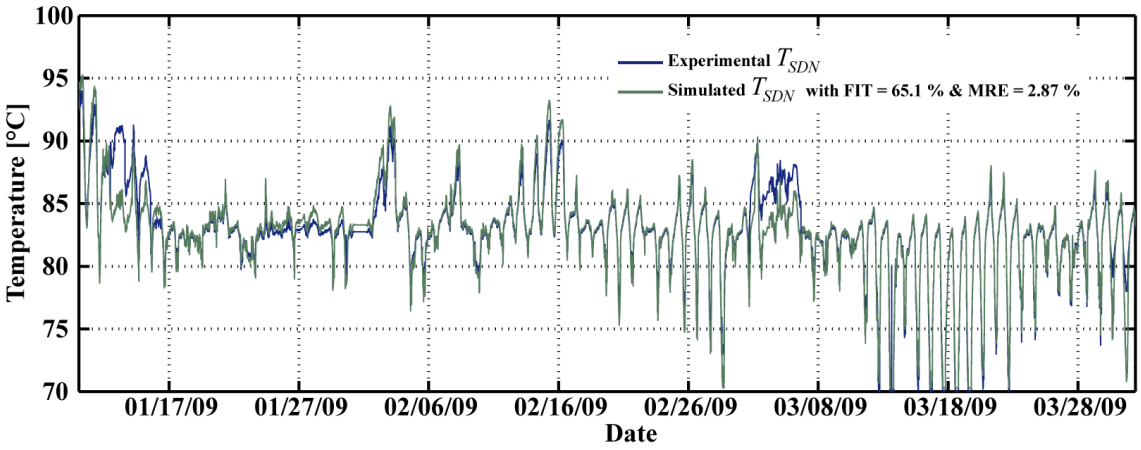

Figure 4. Distribution network set-point temperature.

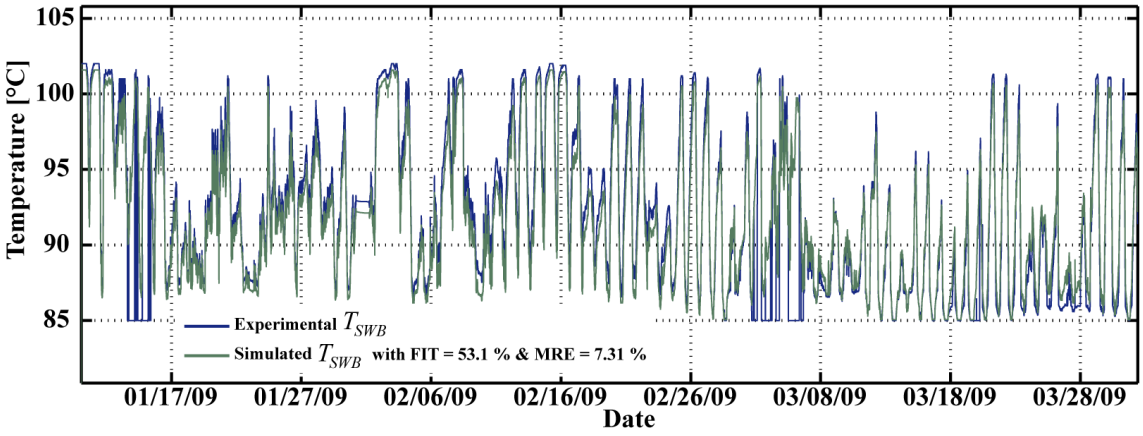

Figure 5. Wood boiler set-point temperature.

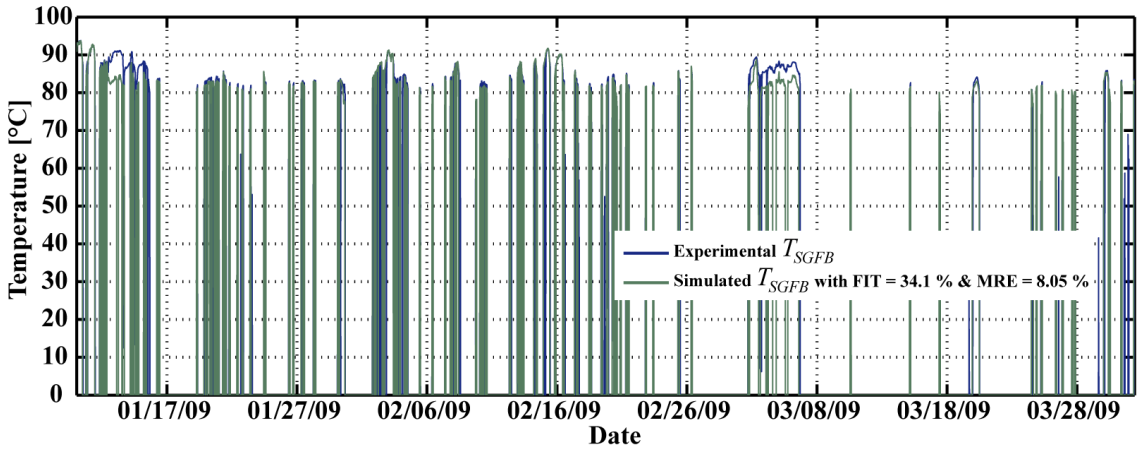

Figure 6. Gas-fuel oil boiler set-point temperature.

Both the FIT and the MRE are about 65% and 3%, 53% and 7% and 34% and 8% for T_{SDN}, T_{SWB} and T_{SC} respectively. Let us note that, because of uncertainty about the way the gas-fuel oil boiler is engaged or stopped (Eng_{GFB}), the results for both the cascade (T_{SC}) and the boiler (T_{SGFB}) (Figure 6) set-point temperatures are not so good, but still consistent.

4.3. Wood boiler

Figure 7 describes the design of the 4.5 MW wood boiler, the way the water passing through the boiler is warmed up (section 4.3.1), as well as all of the parameters used to model its functioning.

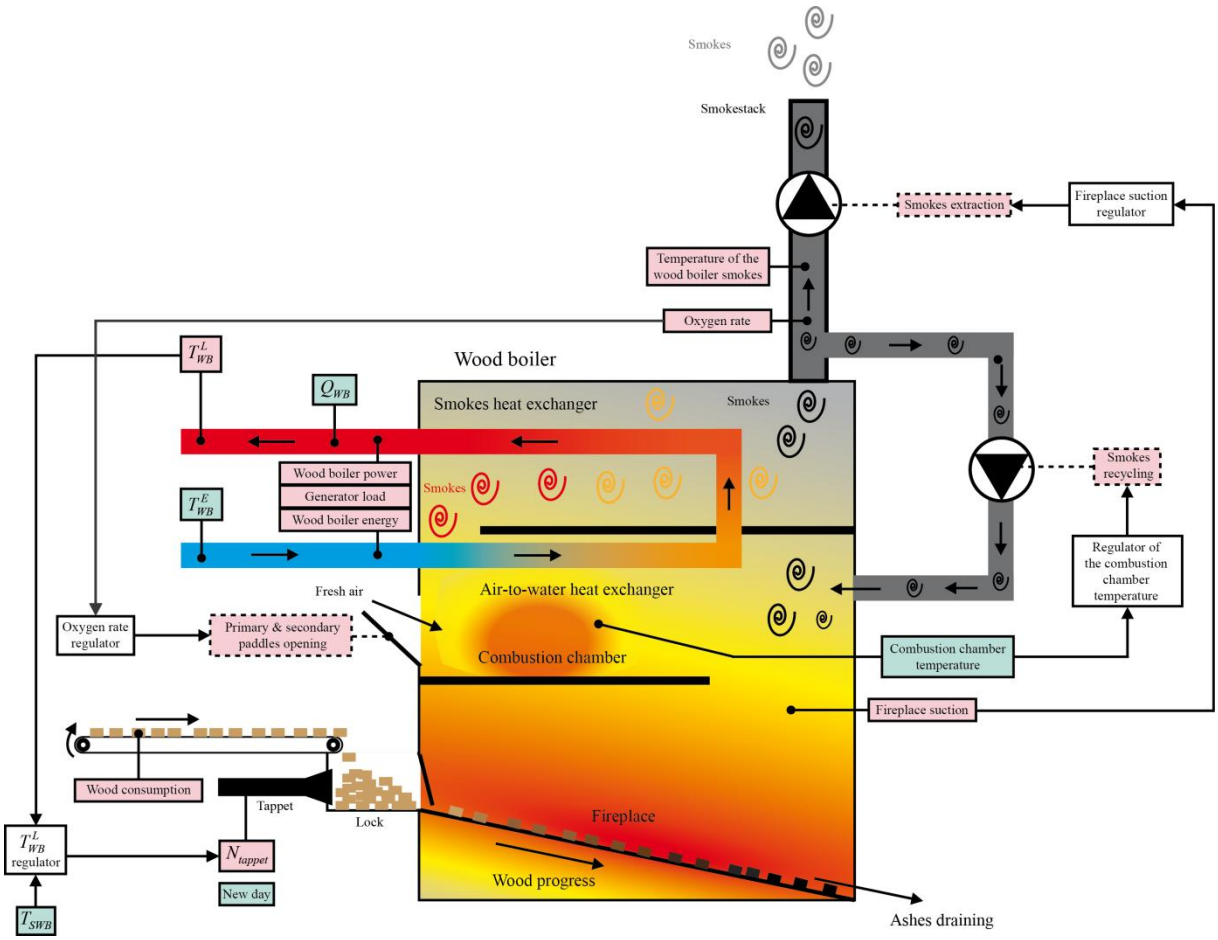

Figure 7. The wood boiler.

4.3.1. Wood boiler working

The wood boiler is the main component of the district boiler of La Rochelle (Figure 7). It uses ground woodchip to heat cold water. Let us note that this wood has to meet criteria such as the size of the pieces, the dust rate or about humidity. However, the wood quality does not remain the same all the time. As a result, this impacts on both the working and the performance of the boiler. The wood pallets come from a silo on a treadmill then are dumped gradually into a lock. Its filling up is done until the wood reaches the desired level, what represents a mean weight of about 37 kg. A tappet allows the wood to enter inside the boiler. As a consequence of this mechanism, the volume of injected wood may vary significantly. Inside the boiler, the wood is burned step-by-step, in both the fireplace and the combustion chamber, and the ashes are removed. The cold water is first warmed up while passing through an air-to-water heat exchanger (in the combustion chamber) then, in a second heat exchanger, using hot smokes, filtered and evacuated through a smokestack. Let us note that the functioning of the wood boiler is impacted by the presence of clinker as well as dirtying. It is also related to the regulation of influential parameters. First, the temperature of the water leaving the boiler is controlled, using a classical PID controller with saturation, to follow the network set-point temperature. A second controller regulates, through a fan used for recycling the smokes, the temperature inside the combustion chamber. Both the temperature set-point and the exact way the controller impacts on the behaviour of the fan are unknown. Next, the oxygen rate in the smokes leaving the boiler is regulated thanks to the opening of shutters (one wants 12% of oxygen in these smokes). Finally, the suction inside the fireplace is regulated around 160 Pa, via the control of a smoke extractor fan. Let us note that all the just-mentioned controllers work separately but are linked one another. Because of the lack of information about these regulations and because many influential parameters are not measured, we focused on the most significant regulation i.e. the regulation of the temperature of the water leaving the boiler and the wood consumption, related to the tappet. As a consequence, we identified a black box Hammerstein-Wiener [30-35] model composed of a linear and two nonlinear blocks (N-L-N) [36]. The model of the wood boiler has four inputs and four outputs. The four inputs are the temperature of the water entering the wood boiler (T_{WB}^{E}), the boiler set-point temperature (T_{SWB}) (section 4.2.2.), the flow of the water passing through the boiler (Q_{WB}) and the parameter Res. Thanks to daily resets (Res), one can calculate both the daily and the cumulative consumptions of wood. The four outputs are the number of tappet strokes per five minutes (N_{tappet}), the just mentioned $Wood_d$ and $Wood_c$ parameters and, finally, the temperature of the water leaving the boiler (T_{WB}^{L}) (Figure 8).

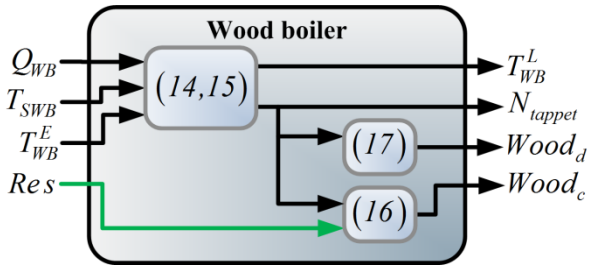

Figure 8. Wood boiler model (in brackets, the model equations).

First, a nonlinear static transformation (a piecewise affine linear function, composed of ten linear pieces, is used), is applied to two (T_{WB}^{E} and T_{SWB}) of the three model inputs (10):

$$\begin{cases} \omega_1 = NL_{PLF}^{10}(T_{WB}^{E}) \\ \omega_2 = NL_{PLF}^{10}(T_{SWB}) \\ \omega_3 = Q_{WB} \end{cases} \quad (10)$$

Because it can only take two values, the flow of the water passing through the boiler does not undergo the transformation. The piecewise affine linear function $NL_{PLF}^{N}(\phi)$ used is defined, $\forall i \in [1, N-1]$, with $a_i = \frac{y_{i+1}-y_i}{x_{i+1}-x_i}$, $b_i = y_i - a_i \times x_i$ and $\delta_i = 1$ if $\phi \in [x_i, x_{i+1}]$, and 0 otherwise (11):

$$\omega = NL_{PLF}^{N}(\phi) = \sum_{i=0}^{N} \left(\delta_i \cdot (a_i \times \phi + b_i)\right) \quad (11)$$

P_i is the break point of coordinates (x_i, y_i), $\forall i \in [1, N]$. The identification process allows finding the right coordinates of these break points. The linear block makes use of ω_1, ω_2 and ω_3 to produce x_1 (12) and x_2 (13), with k the time index:

$$\begin{cases} x_{11}(k) = \sum_{i=1}^{4}\left(\beta_{11,i} \cdot \omega_1(k-i)\right) - \sum_{i=1}^{6}\left(\alpha_{11,i} \cdot x_{11}(k-i)\right) \\ x_{12}(k) = \beta_{12} \cdot \omega_2(k-1) - \alpha_{12} \cdot x_{12}(k-1) \\ x_{13}(k) = \beta_{13} \cdot \omega_3(k-1) - \alpha_{13} \cdot x_{13}(k-1) \\ x_1(k) = x_{11}(k) + x_{12}(k) + x_{13}(k) \end{cases} \tag{12}$$

$$\begin{cases} x_{21}(k) = \sum_{i=1}^{4}\left(\beta_{21,i} \cdot \omega_1(k-i)\right) - \alpha_{21} \cdot x_{21}(k-1) \\ x_{22}(k) = \beta_{22} \cdot \omega_2(k-1) - \sum_{i=1}^{5}\left(\alpha_{22,i} \cdot x_{22}(k-i)\right) \\ x_{23}(k) = \beta_{23} \cdot \omega_3(k-1) - \sum_{i=1}^{5}\left(\alpha_{23,i} \cdot x_{23}(k-i)\right) \\ x_2(k) = x_{21}(k) + x_{22}(k) + x_{23}(k) \end{cases} \tag{13}$$

The second (output) nonlinear block (again a piecewise affine linear function, composed of ten linear pieces, is used) uses x_1 and x_2 to produce the two outputs of the Hammerstein-Wiener model i.e. the number of tappet strokes per five minutes (N_{tappet}) (14) and the temperature of the water leaving the wood boiler (T_{WB}^L) (15):

$$N_{tappet} = NL_{PLF}^{10}(x_1) \tag{14}$$

$$T_{WB}^L = NL_{PLF}^{10}(x_2) \tag{15}$$

4.3.2. Wood consumption

As mentioned in section 4.3.1, both the daily ($Wood_d$) and the cumulative ($Wood_c$) consumptions of wood are deduced from the number of tappet strokes per five minutes (N_{tappet}). The mean weight of the wood introduced into the boiler by the tappet is about 37 kg (W_{wood}). With this volume, one can easily calculate the quantity of wood consumed during one day (16) as well as during the considered period (17), with $Res = 1$ at 6 a.m., and 0 otherwise, and k the time index:

$$Wood_d(k+1) = \left(1 - Res(k)\right) \cdot Wood_d(k) + N_{tappet}(k+1) \times W_{wood} \tag{16}$$

$$Wood_c(k+1) = Wood_c(k) + N_{tappet}(k+1) \times W_{wood} \tag{17}$$

4.3.3. Identification results

Tables 2 to 7 (Appendix) present the results of the Hammerstein-Wiener model identification. Tables 2 (T_{WB}^E) and 3 (T_{SWB}) deal with the parameters of the input nonlinear block. Tables 4 (x_1) and 5 (x_2) are about the parameters of the linear block. Finally, tables 6 (N_{tappet}) and 7 (T_{WB}^L) deal with the parameters of the output nonlinear block. Both the daily ($Wood_d$) (Figure 9) and the cumulative ($Wood_c$) consumptions of wood are well modelled. However, the variability of N_{tappet} and T_{WB}^L (Figure 10) is underestimated (nevertheless the temperature of the water leaving the boiler is well modelled).

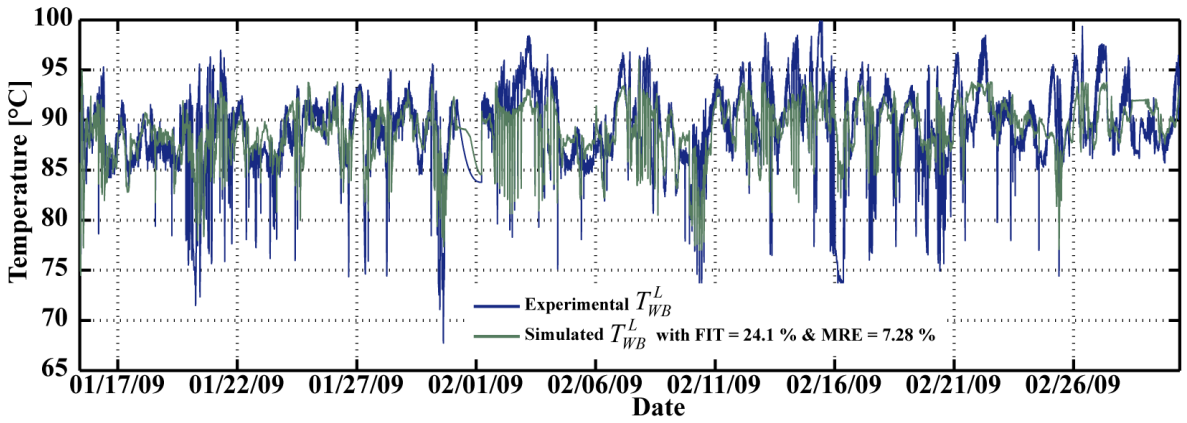

Figure 9. Temperature of the water leaving the wood boiler.

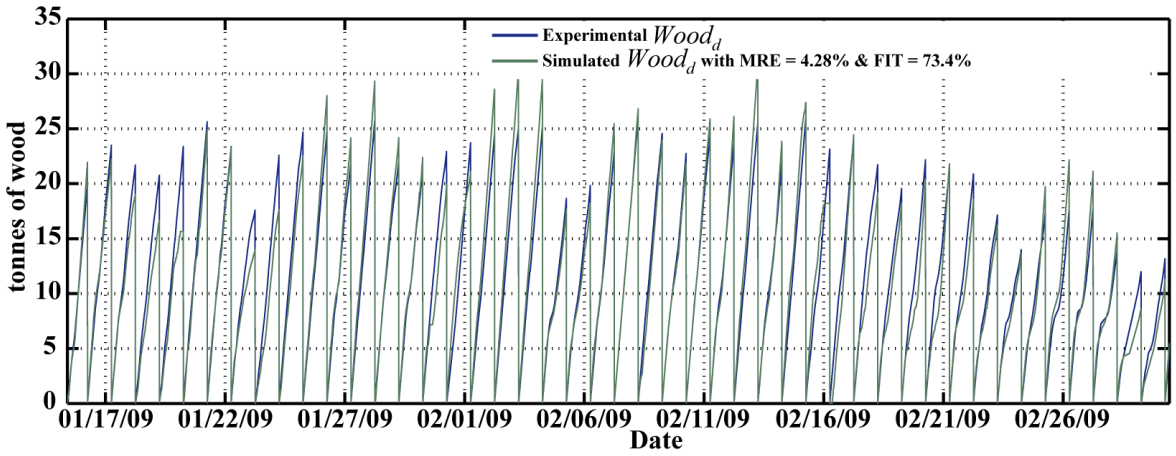

Figure 10. Daily consumption of wood.

One can note that both the FIT and the MRE about 24% and 7% for the temperature of the water leaving the wood boiler (T_{WB}^{L}) and about 73% and 4% for the daily consumption of wood ($Wood_d$).

4.4. Gas-fuel oil boiler

Figure 11 describes the design of the 7 MW gas-fuel oil boiler, the way the water passing through the boiler is warmed up (section 4.4.1), as well as all of the parameters used to model its functioning.

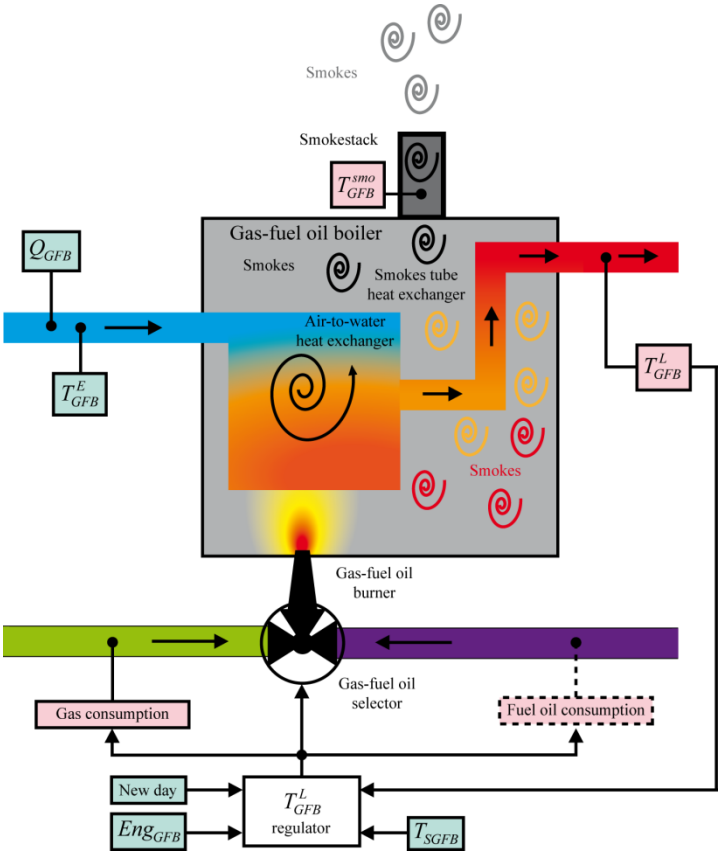

Figure 11. The gas-fuel oil boiler.

4.4.1. Working of the gas-fuel oil boiler

The gas-fuel oil boiler is a 7 MW boiler. As previously mentioned, it functions during very cold periods, only when the wood boiler fails to respond to the hot water demand. Its engaging is related to the difference between T_{SDN} and T_{CHC}^{L} (section 4.2.3). Because a special rate about 6000 m^3 of gas

is allowed every day to Cofely GDF-SUEZ (Gas_d^{max}), gas is first consumed. If the boiler must continue to run, fuel oil is used (in this case gas is much more expensive than fuel oil). The cold water is first warmed up, thanks to the flame of the gas (or fuel oil) burner, while passing through a first air-to-water heat exchanger, then, in a second heat exchanger, using hot smokes. The model of the gas-fuel oil boiler regulator has four inputs and six outputs. The four inputs are the parameter Res (section 4.3.1), the way the boiler is engaged (Eng_{GFB}), the temperature of the water leaving the boiler (T_{GFB}^{L}) as well as the boiler set-point temperature (T_{SGFB}). The six outputs are the real-time ($Gas_{rt}/Fuel_{rt}$), daily ($Gas_d/Fuel_d$) and cumulative ($Gas_c/Fuel_c$) consumptions of gas and fuel oil. In addition, the gas-fuel oil boiler physical model deals with the variations of both the temperature of the water leaving the boiler (T_{GFB}^{L}) and the smokes temperature (T_{GFB}^{smo}), related to the consumption of gas and fuel oil. The model has four inputs, the real-time consumptions of gas (Gas_{rt}) and fuel oil ($Fuel_{rt}$), the way the boiler is engaged (Eng_{GFB}) (section 4.2.3) and the temperature of the water entering the boiler (T_{GFB}^{E}), and the two mentioned outputs (T_{GFB}^{L} and T_{GFB}^{smo}) (Figure 12).

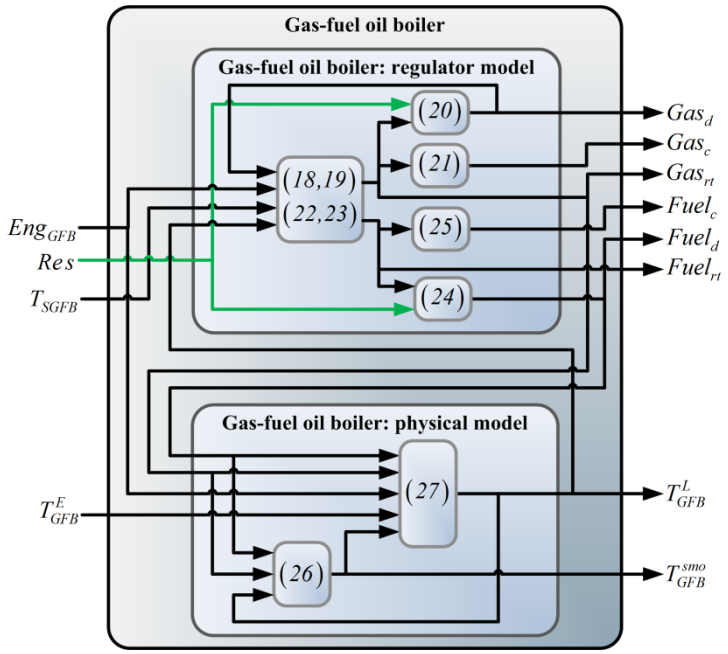

Figure 12. Gas-fuel oil boiler model (in brackets, the model equations).

4.4.2. Gas consumption

The gas consumption is regulated from the difference between the boiler set-point temperature (T_{SGFB}) and the temperature of the water leaving the boiler (T_{GFB}^{L}). Because we do not know how this regulation is carried out, we need to identify all the parameters of the model describing this process. Gas_{rt} is defined as follows, with $\delta Gas_d = 1$ if $Gas_d \leq Gas_d^{max}$ and 0 if $Gas_d > Gas_d^{max}$, $Gas_{rt}^{min} = 0\ m^3.h^{-1}$ and $Gas_{rt}^{max} = 50\ m^3.h^{-1}$ the minimal and maximal volumes of gas usable to feed the burner respectively (19), T_{SGFB} the boiler set-point temperature, T_{GFB}^{L} the temperature of the water leaving the boiler, α^{gas}, β^{gas} and γ^{gas} three parameters to be identified and k the time index (18):

$$Gas_{rt}(k+1) = Eng_{GFB}(k) \cdot \delta Gas_d(k) \cdot \left(\alpha^{gas} \cdot \left(\beta^{gas} \cdot T_{SGFB}(k) - T_{GFB}^{L}(k)\right) + \gamma^{gas}\right) \quad (18)$$

$$\begin{cases} if\ Gas_{rt}(k+1) \geq Gas_{rt}^{max}\ then\ Gas_{rt}(k+1) = Gas_{rt}^{max} \\ if\ Gas_{rt}(k+1) \leq Gas_{rt}^{min}\ then\ Gas_{rt}(k+1) = Gas_{rt}^{min} \\ end\ if \end{cases} \quad (19)$$

The daily volume of gas consumed (Gas_d) is calculated using the parameter Res (to reset Gas_d, every day at 6 a.m.) (section 4.3.1) (20). With this calculation, one can check if the daily volume of gas consumed has reached, or not, 6000 m^3 (Gas_d^{max}). As previously mentioned, when this happens and if the boiler must continue to run to respond to the hot water demand, fuel oil is used:

$$Gas_d(k+1) = (1 - Res) \cdot Gas_d(k) + Gas_{rt}(k+1) \quad (20)$$

Finally, with the calculation of Gas_c (the cumulative consumption of gas), one can observe the consumption evolution during the considered period. This allows validating the proposed model by comparing the real and modelled consumptions of gas (21) during this period:

$$Gas_c(k+1) = Gas_c(k) + Gas_{rt}(k+1) \tag{21}$$

4.4.3. Fuel oil consumption

Due to the lack of information leading to uncertainly about how fuel oil consumption is regulated and because no measurements are carried out at the district boiler of La Rochelle, the way this parameter is modelled is similar to what we have done with gas consumption (section 4.4.2). A transformation coefficient $\delta^{gas-fuel\ oil} = 1.111$ defines the energy ratio between 1 m^3 of gas and 1 litre of fuel oil. With the model, one can estimate the real-time ($Fuel_{rt}$), daily ($Fuel_d$) and cumulative ($Fuel_c$) volumes of fuel oil consumed. Assuming that the gas-fuel oil boiler is producing the same quantity of energy, whatever the combustible used, we developed the model considering the respective high and low heating values of gas (HHV_{gas} and LHV_{gas}) and fuel oil ($HHV_{fuel\ oil}$ and $LHV_{fuel\ oil}$) as well as, for each of the two combustibles, the ratios between these two values. Let us remember that the gross or upper heating value is the amount of heat produced from the complete combustion of a specific amount of combustible. It is obtained when all products of the combustion are cooled down to the temperature before the combustion and when the water vapour formed during combustion is condensed. The net or lower heating value is obtained by subtracting the latent heat of vaporization of the water vapour formed by the combustion from the gross heating value. $Fuel_{rt}$ (22-23) is defined as follows, with Eng_{GFB} the way the boiler is engaged, δGas_d the Boolean parameter defined in section 4.4.2, T_{SGFB} the boiler set-point temperature, T^L_{GFB} the temperature of the water leaving the boiler, $\alpha^{fuel} = \alpha^{gas}$, $\beta^{fuel} = \beta^{gas}$, $\gamma^{fuel} = \gamma^{gas}$, $Fuel^{min}_{rt} = 0\ l.h^{-1}$ and $Fuel^{max}_{rt} = 65\ l.h^{-1}$ the minimal and maximal volumes of fuel oil usable to feed the burner respectively (23) and k the time index:

$$Fuel_{rt}(k+1) = Eng_{GFB}(k) \cdot \left(1 - \delta Gas_d(k)\right) \cdot \delta^{gas-fuel} \cdot \left(\alpha^{fuel} \cdot \left(\beta^{fuel} \cdot T_{SGFB}(k) - T^L_{GFB}(k)\right) + \gamma^{fuel}\right) \tag{22}$$

$$\begin{cases} if\ Fuel_{rt}(k+1) \geq Fuel^{max}_{rt}\ then\ Fuel_{rt}(k+1) = Fuel^{max}_{rt} \\ if\ Fuel_{rt}(k+1) \leq Fuel^{min}_{rt}\ then\ Fuel_{rt}(k+1) = Fuel^{min}_{rt} \\ end\ if \end{cases} \tag{23}$$

Finally, equations (24) and (25) define the daily ($Fuel_d$) and cumulative ($Fuel_c$) consumptions of fuel oil respectively, in the same way we have done with gas consumption:

$$Fuel_d(k+1) = (1 - Res) \cdot Fuel_d(k) + Fuel_{rt}(k+1) \tag{24}$$

$$Fuel_c(k+1) = Fuel_c(k) + Fuel_{rt}(k+1) \tag{25}$$

4.4.4. Smokes temperature

As previously mentioned, after being warmed up while passing through a first air-to-water heat exchanger, the cold water is warmed up again, using the hot smokes which are leaving the gas-fuel oil boiler. As a consequence, one needs first to understand how the smokes temperature (T^{smo}_{GFB}) evolves with the aim of accurately modelling the temperature of the water leaving the boiler (T^L_{GFB}) (section 4.4.5). The smokes temperature (26) is related to the real-time consumption of gas (Gas_{rt}) or fuel oil ($Fuel_{rt}$) and, as just mentioned, to the temperature of the water leaving the boiler. α^{smo}, β^{smo}_1, β^{smo}_2, β^{smo}_3 and γ^{smo} are parameters to be identified and k is the time index:

$$T^{smo}_{GFB}(k+1) = \alpha^{smo} \cdot T^{smo}_{GFB}(k) + \beta^{smo}_1 \cdot T^L_{GFB}(k) + \beta^{smo}_2 \cdot Gas_{rt}(k) + \beta^{smo}_3 \cdot Fuel_{rt}(k) + \gamma^{smo} \tag{26}$$

4.4.5. Temperature of the water leaving the boiler

The temperature of the water leaving the gas-fuel oil boiler (T^L_{GFB}) is given by equation (27), with, as previously mentioned, Eng_{GFB} the way the boiler is engaged, T^E_{GFB} the temperature of the water entering the boiler, T^{smo}_{GFB} the smokes temperature, Gas_{rt} the real-time consumption of gas, $Fuel_{rt}$ the real-time consumption of oil fuel, $\alpha^{T^L_{GFB}}_1$, $\alpha^{T^L_{GFB}}_2$, $\beta^{T^L_{GFB}}_1$, $\beta^{T^L_{GFB}}_2$, $\beta^{T^L_{GFB}}_3$, $\beta^{T^L_{GFB}}_4$, $\beta^{T^L_{GFB}}_5$, $\beta^{T^L_{GFB}}_6$, $\beta^{T^L_{GFB}}_7$ and $\gamma^{T^L_{GFB}}$ the

parameters to be identified and k the time index. Equation (26) allows taking into account the gas-fuel oil boiler dynamics related to its functioning mode (let us remember that this boiler functions during very cold periods only, when the wood boiler fails to respond to the hot water demand):

$$T_{GFB}^{L}(k+1) = \left(\alpha_1^{T_{GFB}^{L}} \cdot Eng_{GFB}(k) + \alpha_2^{T_{GFB}^{L}} \cdot \left(1 - Eng_{GFB}(k)\right)\right) \cdot T_{GFB}^{L}(k) + \beta_1^{T_{GFB}^{L}} \cdot T_{GFB}^{smo}(k) + \gamma^{T_{GFB}^{L}} + \beta_2^{T_{GFB}^{L}} \cdot Gas_{rt} + \beta_3^{T_{GFB}^{L}} \cdot \left(Gas_{rt}(k)\right)^{0.5} + \beta_4^{T_{GFB}^{L}} \cdot Fuel_{rt} + \beta_5^{T_{GFB}^{L}} \cdot \left(Fuel_{rt}(k)\right)^{0.5} + \left(\beta_6^{T_{GFB}^{L}} \cdot Eng_{GFB}(k) + \beta_7^{T_{GFB}^{L}} \cdot \left(1 - Eng_{GFB}(k)\right)\right) \cdot T_{GFB}^{E}(k) \quad (27)$$

4.4.6. Identification results

Table 8 (Appendix) deals with the identification process of the parameters of the gas-fuel oil boiler model. Over-all, the model accuracy can be considered as satisfactory. First, one can highlight that both the daily (Gas_d) (Figure 13) and the cumulative (Gas_c) consumptions of gas are well modelled, even if the modelled real-time consumption of gas (Gas_{rt}) is not so accurate. The temperature of the water leaving the boiler (T_{GFB}^{L}) (Figure 14) is also well modelled, in particular when the boiler is running. If not, the difference between the real and the modelled temperatures of the water leaving the boiler is not significant because this water does not join the collecting hydraulic circuit. Finally, let us note that the model performance is strongly related to the boiler engaging (Eng_{GFB}) which is not easy to model (section 4.2.3). Both the FIT and the MRE are about 76% and 3% for the daily consumption of gas and about 44% and 9% for the temperature of the water leaving the gas-fuel oil boiler.

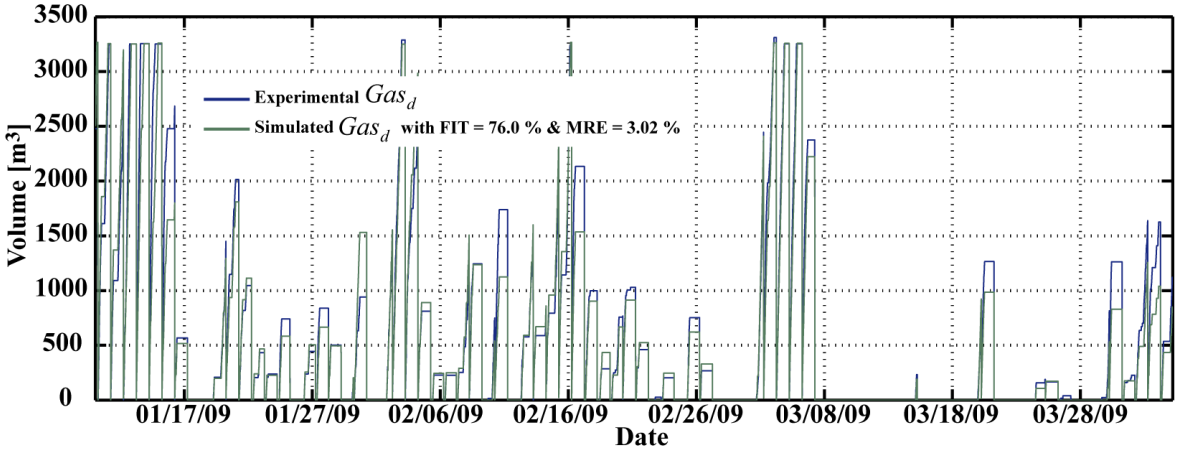

Figure 13. Daily consumption of gas.

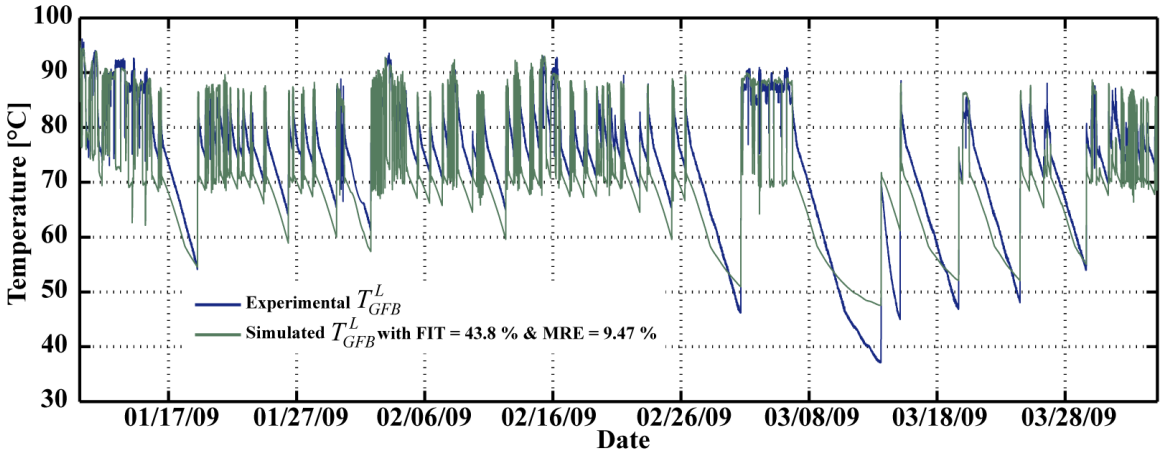

Figure 14. Temperature of the water leaving the gas-fuel oil boiler.

4.5. Collecting hydraulic circuit

The modelling of the collecting hydraulic circuit (Figure 15) deals with both the flow and the temperature of the water passing through the circuit. First, the proposed model describes the thermodynamic behaviour of the water at the "departure" part of the circuit. We modelled the flow of the water passing through both the wood and the gas-fuel oil boilers, knowing which valves are open, and we used this parameter to estimate both the flow and the temperature of the water entering the collecting hydraulic circuit. The proposed model also deals with the thermodynamic behaviour of the water at the "return" part of the circuit. In this sense, we modelled the temperature of the water entering the boilers thanks to both the temperature of the water back from the collecting hydraulic circuit and the flow of the water passing through the boilers. The model of the circuit has five inputs and six outputs (Figure 16). The five inputs are Eng_{WB}, Eng_{GFB}, T^L_{WB}, T^L_{GFB} and T^E_{CHC}. The six outputs are Q_{WB}, Q_{CHC}, Q_{GFB}, T^L_{CHC}, T^E_{GFB} and T^E_{WB}.

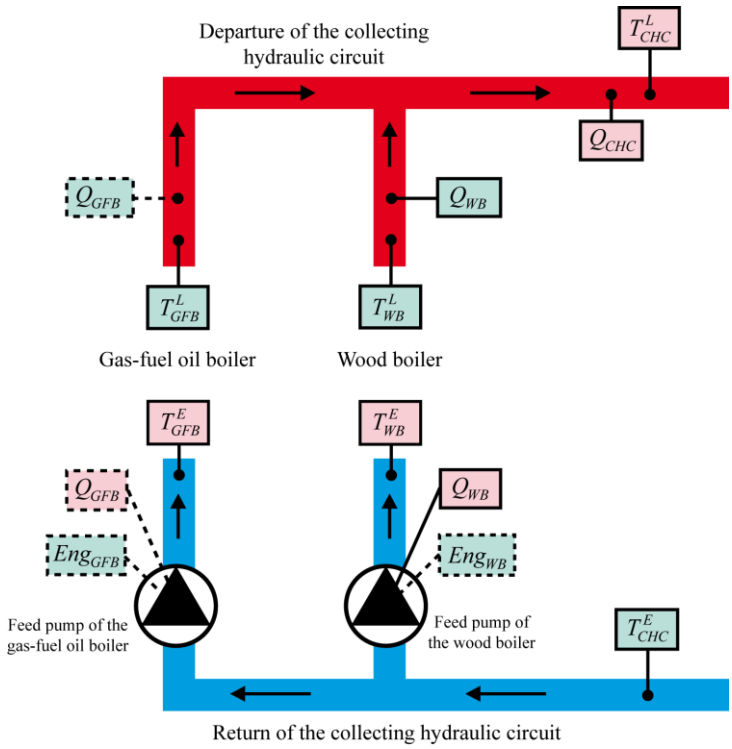

Figure 15. The collecting hydraulic circuit.

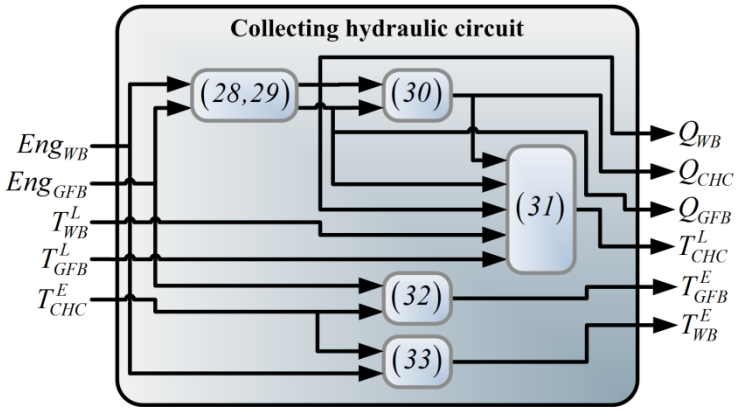

Figure 16. Collecting hydraulic circuit model (in brackets, the model equations).

4.5.1. Flow of the water passing through the gas-fuel oil boiler

First, let us note that, because the sampling time is large in comparison with the time the pump needs to feed the boiler, we do not take into consideration the pump inertia. As a consequence, the

flow of the water passing through the gas-fuel oil boiler (Q_{GFB}) remains *a priori* unchanged when the state of the collecting hydraulic circuit is stable. When the gas-fuel oil boiler works alone (i.e. $Eng_{GFB} = 1$ while $Eng_{WB} = 0$), its nominal flow is about 344 m^3.h^{-1} ($Q_{GFB}^{Nom_1}$). When the two boilers work at the same time ($Eng_{GFB} = 1$ and $Eng_{WB} = 1$), this nominal flow is about 319 m^3.h^{-1} ($Q_{GFB}^{Nom_2}$). Algebraic equation (28) describes the way the flow of the water passing through the gas-fuel oil boiler has been modelled, with Eng_{GFB} and Eng_{WB} describing the way the two boilers are engaged or stopped:

$$Q_{GFB} = Eng_{GFB} \cdot \left(Q_{GFB}^{Nom_1} - \left(Q_{GFB}^{Nom_1} - Q_{GFB}^{Nom_2}\right) \cdot Eng_{WB}\right) \tag{28}$$

4.5.2. Flow of the water passing through the wood boiler

Again, and because the sampling time is large in comparison with the time the pump needs to feed the boiler, we do not take into consideration the pump inertia. As a result, the flow of the water passing through the wood boiler (Q_{WB}) remains *a priori* unchanged when the state of the collecting hydraulic circuit is stable. When the wood boiler works alone (i.e. $Eng_{WB} = 1$ while $Eng_{GFB} = 0$), its nominal flow is about 265 m^3.h^{-1} ($Q_{WB}^{Nom_1}$). When the two boilers work at the same time (i.e. $Eng_{WB} = 1$ and $Eng_{GFB} = 1$), this nominal flow is about 246 m^3.h^{-1} ($Q_{WB}^{Nom_2}$). Algebraic equation (29) describes the way the flow of the water passing through the wood boiler has been modelled, in the same way we have done with Q_{GFB}:

$$Q_{WB} = Eng_{WB} \cdot \left(Q_{WB}^{Nom_1} - \left(Q_{WB}^{Nom_1} - Q_{WB}^{Nom_2}\right) \cdot Eng_{GFB}\right) \tag{29}$$

4.5.3. Flow and temperature of the water leaving the collecting hydraulic circuit

The water leaving the collecting hydraulic circuit is the mix of the water leaving the gas-fuel oil boiler and the water leaving the wood boiler. As a consequence, its flow ($Q_{CHC} = Q_{CHC}^E = Q_{CHC}^L$) is equal to the sum of Q_{WB} (the flow of the water passing through the wood boiler) and Q_{GFB} (the flow of the water passing through the gas-fuel oil boiler) (30). Its temperature (T_{CHC}^L) is of course dependent on T_{WB}^L (the temperature of the water leaving the wood boiler) and on T_{GFB}^L (the temperature of the water leaving the gas-fuel oil boiler). It can be expressed as the weighted mean of T_{WB}^L (to which is assigned Q_{WB}) and T_{GFB}^L (to which is assigned Q_{GFB}) compared with Q_{CHC} (31):

$$Q_{CHC} = Q_{WB} + Q_{GFB} \tag{30}$$

$$T_{CHC}^L = \frac{T_{WB}^L \cdot Q_{WB} + T_{GFB}^L \cdot Q_{GFB}}{Q_{CHC}} \tag{31}$$

4.5.4. Temperature of the water entering the gas-fuel oil boiler

The cold water entering the gas-fuel oil boiler is the water back from the collecting hydraulic circuit. If the boiler is working ($Eng_{GFB} = 1$), its temperature (T_{GFB}^E) is almost the same (the slightly difference is due to thermal losses in the tubing) as the temperature of the water entering the collecting hydraulic circuit (T_{CHC}^E). If not ($Eng_{GFB} = 0$), a water gate separates the boiler from the circuit and, as a consequence, T_{GFB}^E (in this case, this is the temperature of the residual water present in the lock) decreases slightly. The proposed model deals with a first-order dynamics when the gas-fuel oil boiler works (allowing adapting T_{GFB}^E to T_{CHC}^E) while it deals with a third-order dynamics when the boiler is stopped ($T_{GFB}^E \to T_{DB}$, with $T_{DB} = 30°C$ the district boiler ambient temperature). As a result, one can model the way T_{GFB}^E is evolving, using the following logical (differential) equations (32), with Eng_{GFB} the way the gas-fuel oil boiler is engaged or stopped, $\alpha_1^{T_{GFB}^E}$, $\alpha_2^{T_{GFB}^E}$, $\alpha_3^{T_{GFB}^E}$, $\alpha_4^{T_{GFB}^E}$, $\alpha_5^{T_{GFB}^E}$, $\alpha_6^{T_{GFB}^E}$, $\beta_1^{T_{GFB}^E}$ and $\delta_1^{T_{GFB}^E}$ the parameters to be identified and k the time index:

$$\begin{cases} T_{GFB}^E(k+1) = Eng_{GFB} \cdot \left(\alpha_1^{T_{GFB}^E} \cdot T_{GFB}^E(k) + \beta_1^{T_{GFB}^E} \cdot T_{CHC}^E(k)\right) + (1 - Eng_{GFB}) \cdot \left(T_{GFB}^E(k) + \alpha_2^{T_{GFB}^E} \cdot x_2^{T_{GFB}^E}(k)\right) \\ x_2^{T_{GFB}^E}(k+1) = (1 - Eng_{GFB}) \cdot \left(x_2^{T_{GFB}^E}(k) + \alpha_3^{T_{GFB}^E} \cdot x_3^{T_{GFB}^E}(k)\right) \\ x_3^{T_{GFB}^E}(k+1) = (1 - Eng_{GFB}) \cdot \left(\alpha_4^{T_{GFB}^E} \cdot T_{GFB}^E(k) + \alpha_5^{T_{GFB}^E} \cdot x_2^{T_{GFB}^E}(k) + \alpha_6^{T_{GFB}^E} \cdot x_3^{T_{GFB}^E}(k) + \delta_1^{T_{GFB}^E}\right) \end{cases} \tag{32}$$

4.5.5. Temperature of the water entering the wood boiler

The cold water entering the wood boiler is the water back from the collecting hydraulic circuit. If the boiler is working ($Eng_{WB} = 1$), its temperature (T^E_{WB}) is almost the same as the temperature of the water entering the collecting hydraulic circuit (T^E_{CHC}) (again, the slightly difference between the two temperatures is due to thermal losses and inertia). The model proposed deals with two different first-order dynamics when the gas-fuel boiler works (allowing adapting T^E_{WB} to T^E_{CHC}) and when it is stopped ($T^E_{WB} \rightarrow T_{DB}$, with $T_{DB} = 30°C$ the district boiler ambient temperature). As a result, one can model the way T^E_{WB} is evolving, using logical (differential) equation (33), with Eng_{WB} the way the wood boiler is engaged or stopped, $\alpha_1^{T^E_{WB}}$, $\alpha_2^{T^E_{WB}}$ and $\beta_1^{T^E_{WB}}$ the parameters to be identified and k the time index:

$$T^E_{WB}(k+1) = Eng_{WB} \cdot \left(\alpha_1^{T^E_{WB}} \cdot T^E_{WB}(k) + \beta_1^{T^E_{WB}} \cdot T^E_{CHC}(k)\right) + (1 - Eng_{WB}) \cdot \left(\alpha_2^{T^E_{WB}} \cdot T^E_{WB}(k) + \left(1 - \alpha_2^{T^E_{WB}}\right) \cdot T_{DB}\right) \quad (33)$$

4.5.6. Identification results

Table 9 (Appendix) deals with the identification process about the parameters of the collecting hydraulic circuit model. Let us remember that no parameters have to be identified for Q_{GFB}, Q_{WB}, Q_{CHC} and T^L_{CHC}. Over-all, the model accuracy is good. One can highlight that, when the gas-fuel oil boiler is stopped, T^E_{GFB} is not well estimated. However, and because in this case the boiler is separated from the rest of the plant, this is not significant (as previously mentioned, the residual water present in the lock is not mixed with the water passing through the plant). Moreover, when the gas-fuel oil boiler works again, the model convergence is very fast, whatever the difference between the real and estimated values of T^E_{GFB} when the gas-fuel oil boiler is stopped. Both the FIT and the MRE are about 74% and 2% for the temperature of the water leaving the collecting hydraulic circuit (Figure 17) and about 93% and 0.5% for its flow (Figure 18).

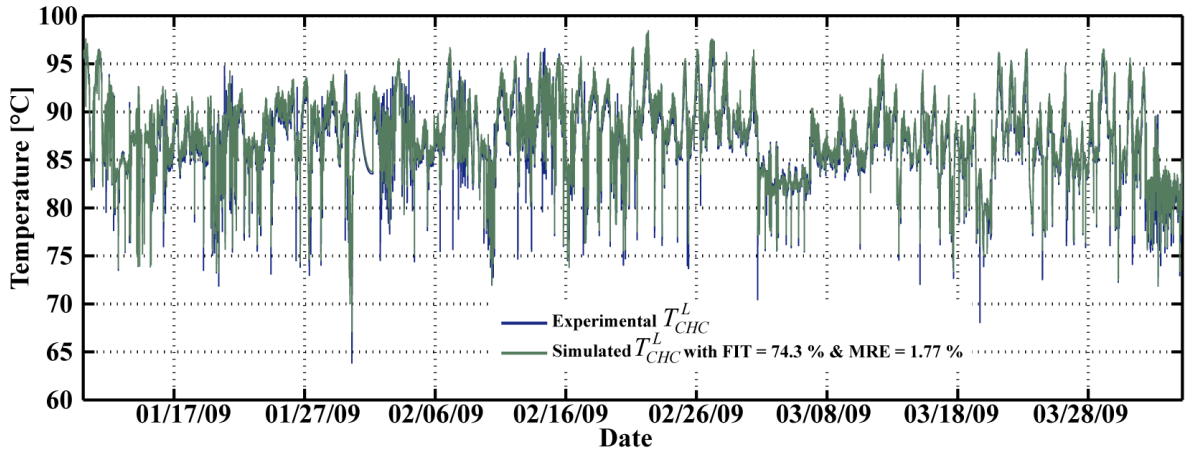

Figure 17. Temperature of the water leaving the collecting hydraulic circuit.

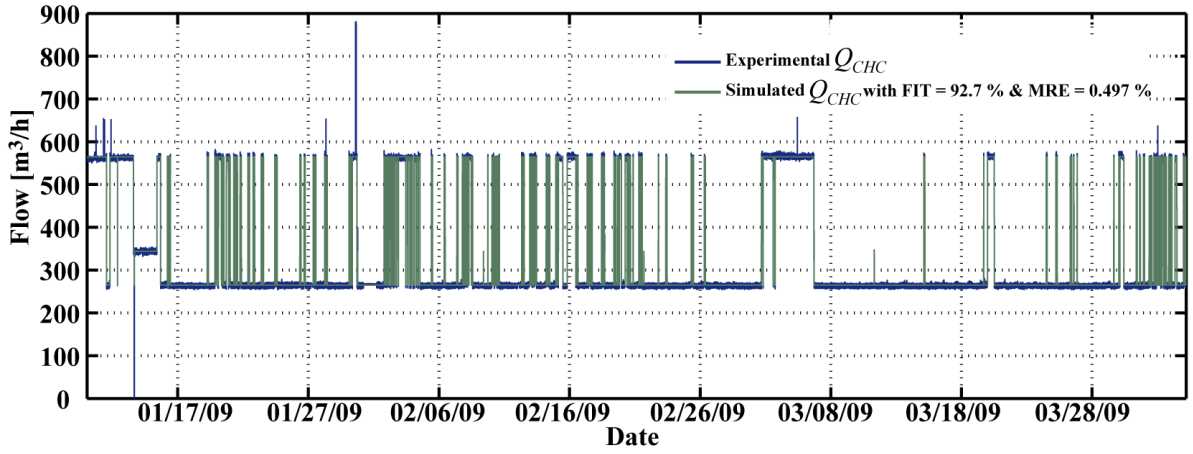

Figure 18. Flow of the water passing through the collecting hydraulic circuit.

4.6. Breaking pressure bottle

A breaking pressure bottle allows connecting two hydraulic circuits whose flows, fixed by pumps, are different. At the district boiler of La Rochelle, the bottle connects both the primary and the collecting hydraulic circuits (section 2) by recycling a part of the water passing through the circuit whose flow is the larger (Figure 19). Let us note that the flow of the water passing through the collecting hydraulic circuit (section 4.5) is related to the way the wood and the gas-fuel oil boilers function (the wood boiler functions alone except when it fails to respond to the hot water demand, during very cold periods) while the flow of the water passing through the primary hydraulic circuit is dependent on outdoor temperature (section 4.7). Let us also note that the temperature of the water entering the breaking pressure bottle is unknown. Indeed, a part of the cold water coming back from the distribution network is warmed up by the cogeneration plant, before it reaches the bottle.

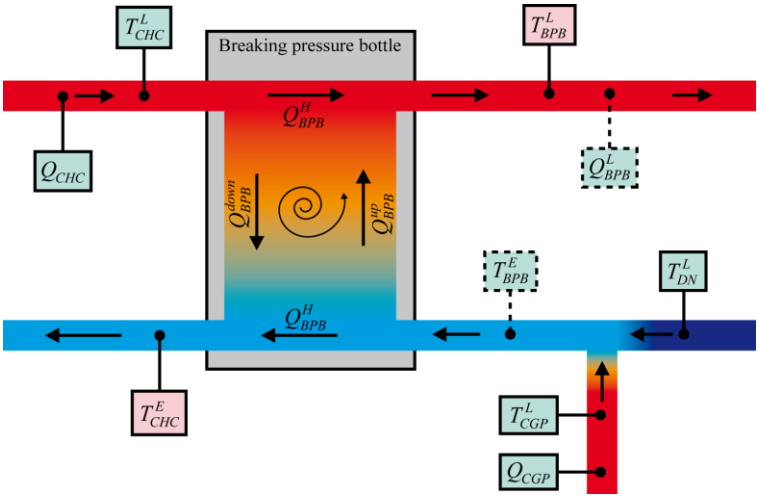

Figure 19. The breaking pressure bottle.

The model of the breaking pressure bottle has six inputs and six outputs. The six inputs are the temperature and the flow of the water leaving the collecting hydraulic circuit (T^L_{CHC} and Q_{CHC}), the temperature and the flow of the water leaving the cogeneration plant (T^L_{CGP} and Q_{CGP}), the temperature of the water back from the distribution network (T^L_{DN}) and the flow of the water leaving the breaking pressure bottle and joining the distribution network (Q^L_{BPB}). The six model outputs are the temperature of the water entering the collecting hydraulic circuit (T^E_{CHC}), the temperature of the water leaving the breaking pressure bottle and joining the distribution network (T^L_{BPB}), the temperature of the water entering the bottle (T^E_{BPB}) as well as both the horizontal (Q^H_{BPB}) and vertical (Q^{up}_{BPB} and Q^{down}_{BPB}) flows inside this bottle (Figure 20).

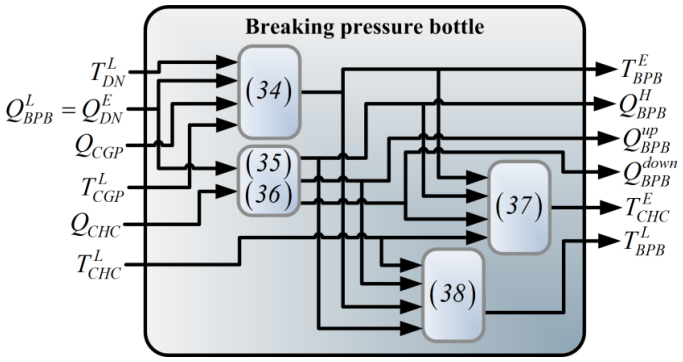

Figure 20. Breaking pressure bottle model (in brackets, the model equations).

4.6.1. Temperature of the water entering the breaking pressure bottle

As just mentioned, the water entering the breaking pressure bottle is coming back from the distribution network after being partially warmed up by the cogeneration plant. Its temperature (T^E_{BPB}) is not measured at the district boiler but is expressed, using algebraic equation (34), as the

mean of the temperature of the cold water coming back directly from the distribution network (T_{DN}^{L}) and the temperature of the water warmed up by the cogeneration plant (T_{CGP}^{L}), weighted by their respective flows:

$$T_{BPB}^{E} = \frac{T_{DN}^{L} \cdot (Q_{BPB}^{L} - Q_{CGP}) + T_{CGP}^{L} \cdot Q_{CGP}}{Q_{BPB}^{L}} \tag{34}$$

4.6.2. Horizontal and vertical flows inside the breaking pressure bottle

One needs to understand the way the water is recycled by the breaking pressure bottle, i.e. to understand how the water circulates vertically and horizontally inside the bottle as well as the way Q_{CHC} and Q_{BPB}^{L} impact on this circulation, to correctly estimate the temperature of the water leaving the bottle and joining the distribution network (T_{BPB}^{L}). Let us note that $Q_{BPB}^{up} \neq 0$ (the updraft flow) when $Q_{BPB}^{L} > Q_{CHC}$ while $Q_{BPB}^{down} \neq 0$ (the downdraft flow) when $Q_{BPB}^{L} < Q_{CHC}$. The horizontal flow (Q_{BPB}^{H}) can be expressed (35) as the minimum of Q_{BPB}^{L} and Q_{CHC} while one can estimate Q_{BPB}^{up} and Q_{BPB}^{down} from the difference between Q_{BPB}^{L} and Q_{CHC}, using logical (algebraic) equations (36):

$$Q_{BPB}^{H} = min(Q_{BPB}^{L}, Q_{CHC}) \tag{35}$$

$$\begin{cases} \delta_{Q_{BPB}^{V}} = (Q_{BPB}^{L} - Q_{CHC}) \geq 0 \\ Q_{BPB}^{up} = \delta_{Q_{BPB}^{V}} \cdot (Q_{BPB}^{L} - Q_{CHC}) \\ Q_{BPB}^{down} = \left(1 - \delta_{Q_{BPB}^{V}}\right) \cdot (Q_{CHC} - Q_{BPB}^{L}) \end{cases} \tag{36}$$

4.6.3. Temperature of the water entering the collecting hydraulic circuit

A part of the water leaving the breaking pressure bottle enters the collecting hydraulic circuit. This water is a mix of the cold water coming back from the distribution network and partially warmed up by the cogeneration plant and, according to the way the breaking pressure bottle recycles water (section 4.6), a part of the hot water leaving the collecting hydraulic circuit. As a consequence, the temperature of the water entering the collecting hydraulic circuit (T_{CHC}^{E}) can be expressed, using algebraic equation (37), as the mean of T_{BPB}^{E} and T_{CHC}^{L}, weighted by Q_{BPB}^{H} (the horizontal flow inside the bottle) and Q_{BPB}^{down} (the downdraft flow inside the bottle) respectively:

$$T_{CHC}^{E} = \frac{T_{BPB}^{E} \cdot Q_{BPB}^{H} + T_{CHC}^{L} \cdot Q_{BPB}^{down}}{Q_{BPB}^{H} + Q_{BPB}^{down}} \tag{37}$$

4.6.4. Temperature of the water leaving the breaking pressure bottle

The water leaving the breaking pressure bottle is a mix of the hot water leaving the collecting hydraulic circuit (and entering the bottle) and, according to the way the breaking pressure bottle recycles water (section 4.6), a part of the water entering this bottle and coming back from the distribution network after being partially warmed up by the cogeneration plant. Consequently, the temperature of the water leaving the breaking pressure bottle and joining the distribution network (T_{BPB}^{L}) can be expressed, using algebraic equation (38), as the mean of T_{CHC}^{L} and T_{BPB}^{E}, weighted by Q_{BPB}^{up} (the updraft flow inside the bottle) and Q_{BPB}^{H} (the horizontal flow inside the bottle) respectively:

$$T_{BPB}^{L} = \frac{T_{CHC}^{L} \cdot Q_{BPB}^{up} + T_{BPB}^{E} \cdot Q_{BPB}^{H}}{Q_{BPB}^{H} + Q_{BPB}^{down}} \tag{38}$$

4.6.5. Modelling results

Analyzing the results obtained, one can note that both the temperature of the water leaving the breaking pressure bottle and joining the distribution network (T_{BPB}^{L}) (Figure 21) and the temperature of the water leaving the breaking pressure bottle and entering the collecting hydraulic circuit (T_{CHC}^{E}) (Figure 22) are well modelled. Both the FIT and the MRE are about 67% and 3% for T_{BPB}^{L} and about 58% and 3.5% for T_{CHC}^{E}. The way the water is recycled by the breaking pressure bottle, i.e. the way the water circulates vertically and horizontally inside the bottle, is correctly described by the proposed equations (35 and 36).

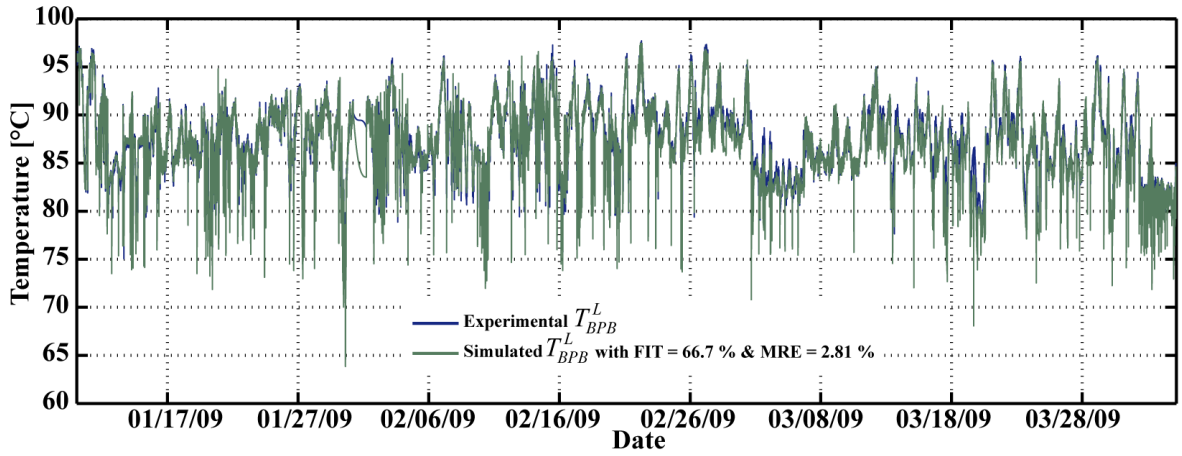

Figure 21. Temperature of the water leaving the breaking pressure bottle.

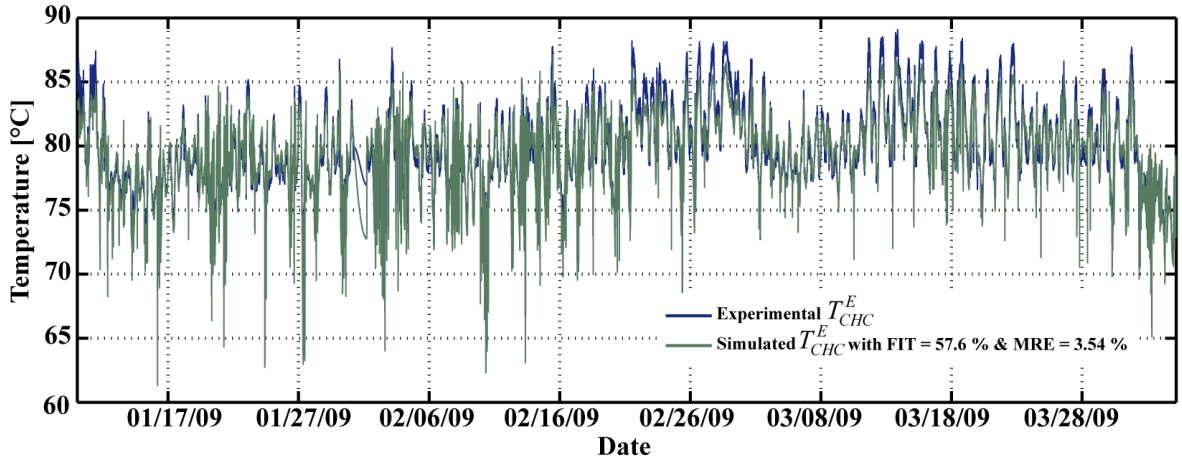

Figure 22. Temperature of the water entering the collecting hydraulic circuit.

4.7. Hot water distribution network

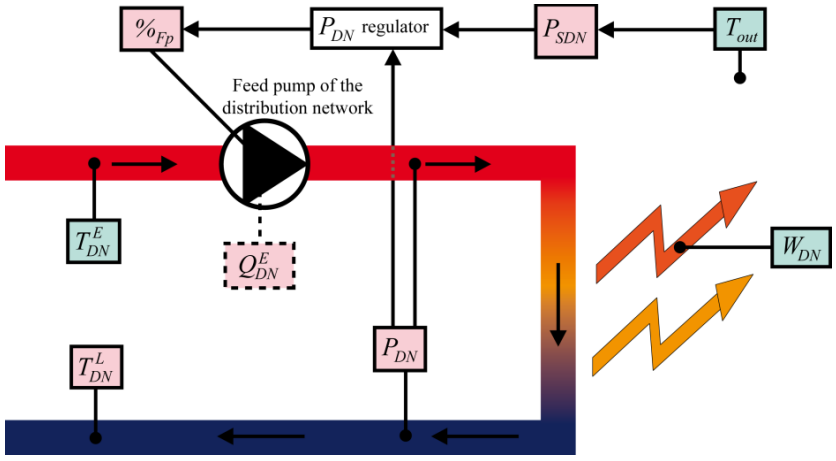

Figure 23. The hot water distribution network.

The flow of the water entering the distribution network (Q^E_{DN}) is regulated. To be sharply exact, this parameter is indirectly controlled. Indeed, one regulates the water differential pressure (P_{DN}) (i.e. the difference between the pressure of the water entering the distribution network and the pressure of the water leaving it) using a feed pump and following a set-point (P_{SDN}) dependent on outdoor temperature. During low outdoor temperatures, power consumption increases. Because

power consumption and Q_{DN}^{E} are proportional, one increases Q_{DN}^{E} and, as a consequence, the water differential pressure, to increase the power supplied (Figure 23). The proposed model has three inputs and five outputs (Figure 24). The three inputs are T_{out}, T_{DN}^{E} and W_{DN}. The five outputs are P_{SDN}, P_{DN}, $\%_{fp}$, Q_{DN}^{E} and T_{DN}^{L}.

4.7.1. Water differential pressure set-point

As just mentioned, the water differential pressure set-point (P_{SDN}) is defined according to outdoor temperature. This parameter is modelled using the following equation system (39), given that, if outdoor temperature is lower than T_{out}^{low}, P_{SDN} is set to 1.1 bars (P_{SDN}^{up}), while it is set to 0.85 bars (P_{SDN}^{low}) when outdoor temperature is upper than T_{out}^{up}. If $T_{out}^{low} \leq T_{out} \leq T_{out}^{up}$, the water differential pressure set-point varies linearly between P_{SDN}^{up} and P_{SDN}^{low}.

$$\begin{cases} C_1^{P_{SDN}} = T_{out} \leq T_{out}^{low} \\ C_2^{P_{SDN}} = T_{out} \geq T_{out}^{up} \\ C_3^{P_{SDN}} = (T_{out} \geq T_{out}^{low}) \wedge (T_{out} \leq T_{out}^{up}) \\ a^{P_{SDN}} = \dfrac{P_{SDN}^{up} - P_{SDN}^{low}}{T_{out}^{low} - T_{out}^{up}} \\ b^{P_{SDN}} = P_{SDN}^{up} - a^{P_{SDN}} \cdot T_{out}^{low} \\ P_{SDN} = C_1^{P_{SDN}} \cdot P_{SDN}^{low} + C_2^{P_{SDN}} \cdot P_{SDN}^{up} + C_3^{P_{SDN}} \cdot (a^{P_{SDN}} \cdot T_{out} + b^{P_{SDN}}) \end{cases} \quad (39)$$

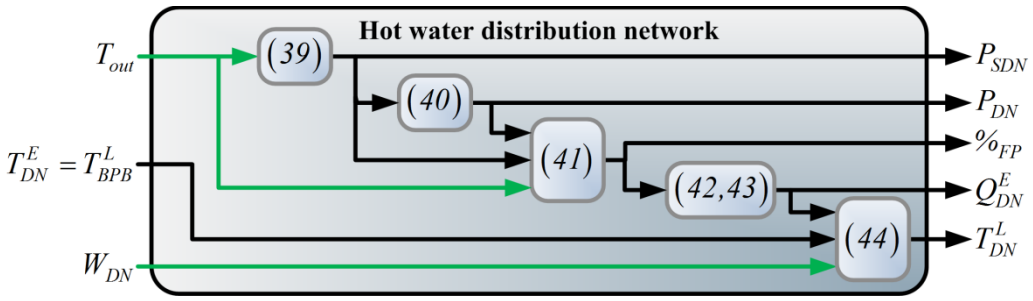

Figure 24. Hot water distribution network model (in brackets, the model equations).

4.7.2. Water differential pressure

This parameter is well regulated and, as a consequence, closely follows the set-point (section 4.7.1). However, measurements are affected by noise whose origin is unidentified. To avoid the identification of the (unknown) regulation process, we modelled the considered parameter in a simple way, using the differential pressure set-point (40):

$$P_{DN} = P_{SDN} \quad (40)$$

4.7.3. Working of the distribution network feed pump

A feed pump controls the amount of water entering the distribution network, discharging a variable flow. Without any measurements of this flow, we modelled the pump working using the opening percentage of its valve ($\%_{fp}$) which is fixed according to the water differential pressure. As a consequence, the feed pump working can be expressed as follows, using equation (41), with P_{DN} the water differential pressure, P_{SDN} the differential pressure set-point, T_{out} the outdoor temperature, α^{fp}, β_1^{fp}, β_2^{fp}, β_3^{fp} and γ^{fp} the parameters to be identified and k the time index:

$$\%_{fp}(k+1) = \alpha^{fp} \cdot \%_{fp}(k) + \beta_1^{fp} \cdot P_{SDN}(k) + \beta_2^{fp} \cdot T_{out}(k) + \beta_3^{fp} \cdot P_{DN}(k) + \gamma^{fp} \quad (41)$$

4.7.4. Flow of the water entering the distribution network

The flow of the water entering the distribution network ($Q_{DN}^{E} = Q_{BPB}^{L}$) is unfortunately not measured. This is one of the main drawbacks of the proposed model because this parameter

impacts on the calculation of both the thermal power consumption and the flow repartition inside the breaking pressure bottle. However, Cofely GDF-SUEZ did some investigations to correlate Q_{DN}^{E} and the water differential pressure (P_{DN}). As a consequence, we decided first to interpolate the data collected with the aim of modelling the considered parameter (Q_{DN}^{E}). Unfortunately, these data are insufficient to obtain good results. That is why we used also the opening percentage of the feed pump valve ($\%_{fp}$). So, Q_{DN}^{E} can be expressed as follows, using equation (42), with $\beta^{Q_{DN}^{E}}$ and $\gamma^{Q_{DN}^{E}}$ two parameters to be identified and k the time index:

$$Q_{DN}^{E}(k+1) = \beta^{Q_{DN}^{E}} \cdot \left(\%_{fp}(k)\right)^{2} + \gamma^{Q_{DN}^{E}} \tag{42}$$

As a key point, one can note that after identifying the parameters of equation (42) (Table 10), we used the values of Q_{DN}^{E} we obtained to improve the modelling of the breaking pressure bottle (one of the influent flows was not correctly estimated). Moreover, the flow of the water leaving the collecting hydraulic circuit allowed highlighting that Q_{DN}^{E} was overestimated. As a result, it has to undergo a linear transformation to minimize the difference between the real and modelled flows of the water leaving the breaking pressure bottle (43), with $\eta^{Q_{DN}^{E}}$ and $\kappa^{Q_{DN}^{E}}$ two parameters to be identified:

$$Q_{DN}^{E} = \eta^{Q_{DN}^{E}} \cdot Q_{DN}^{E} + \kappa^{Q_{DN}^{E}} \tag{43}$$

4.7.5. Temperature of the water leaving the distribution network

The temperature of the cold water coming back directly from the distribution network (T_{DN}^{L}) can be expressed, using equation (44), as the difference between the temperature of the water entering the distribution network (T_{DN}^{E}) and a term defined according to the thermal power consumed by the hot water distribution network (W_{DN}), the flow of the water entering this network (Q_{DN}^{E}) as well as both the density ($\rho_{water} = 971.6\ kg.m^{-3}$) and the specific heat capacity ($Cp_{water} = 4196\ J.kg^{-1}.K^{-1}$) of water. Because no energy meter is currently installed at the district boiler of La Rochelle, W_{DN} has been estimated:

$$T_{DN}^{L} = T_{DN}^{E} - \frac{W_{DN} \cdot 3600}{Q_{DN}^{E} \cdot \rho_{water} \cdot Cp_{water}} \tag{44}$$

4.7.6. Identification results

Table 10 (Appendix) deals with the identification process of the parameters of the hot water distribution network model. Over-all, the model accuracy can be considered as satisfactory. Let us note that no parameters have to be identified for the thermal power consumption (W_{DN}) and the temperature of the water leaving the distribution network (T_{DN}^{L}). Figures 25 and 26 depict the modelling of both the water differential pressure (P_{DN}) and the opening percentage of the distribution network feed pump ($\%_{fp}$). Both the FIT and the MRE are about 66% and 3.5% for P_{DN} and about 64% and 4% for $\%_{fp}$. Let us remember that $\%_{fp}$ is a significant parameter, used to model the flow of the water entering the distribution network (Q_{DN}^{E}).

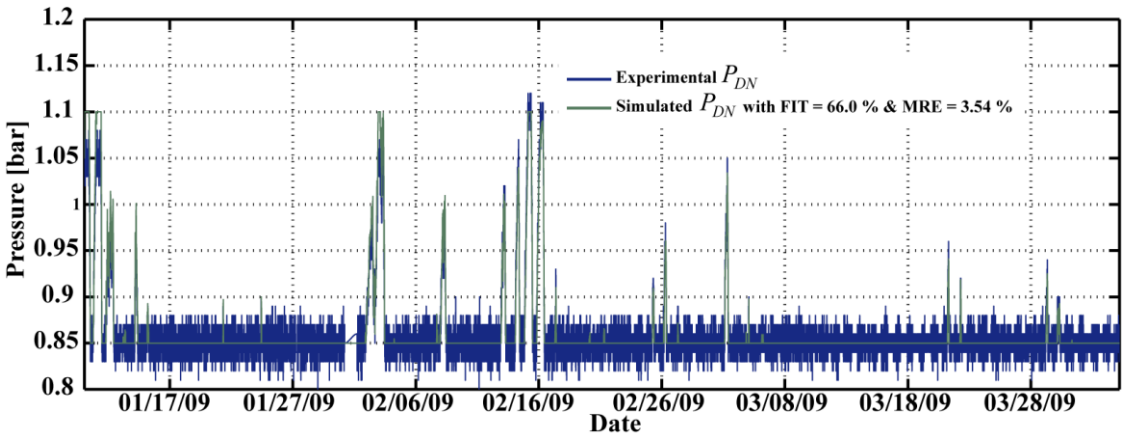

Figure 25. Water differential pressure.

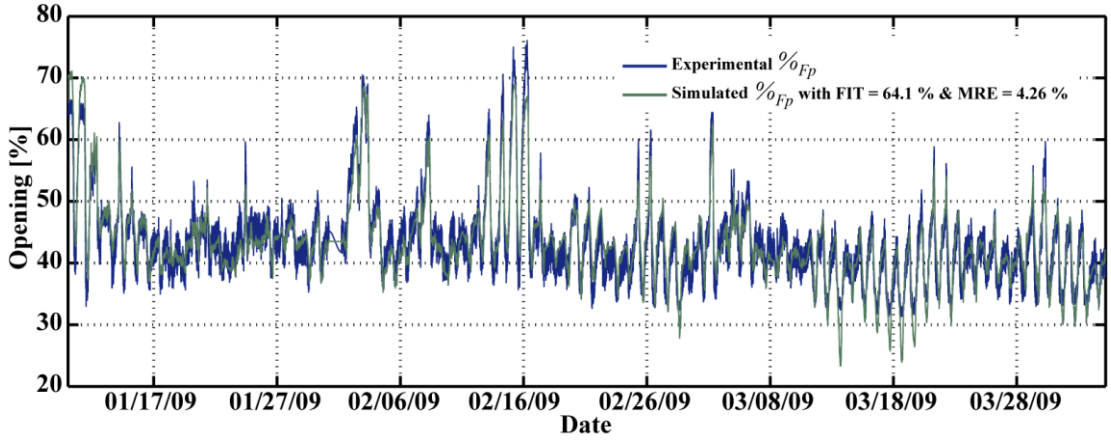

Figure 26. Opening percentage of the distribution network feed pump.

4.8. Cogeneration plant

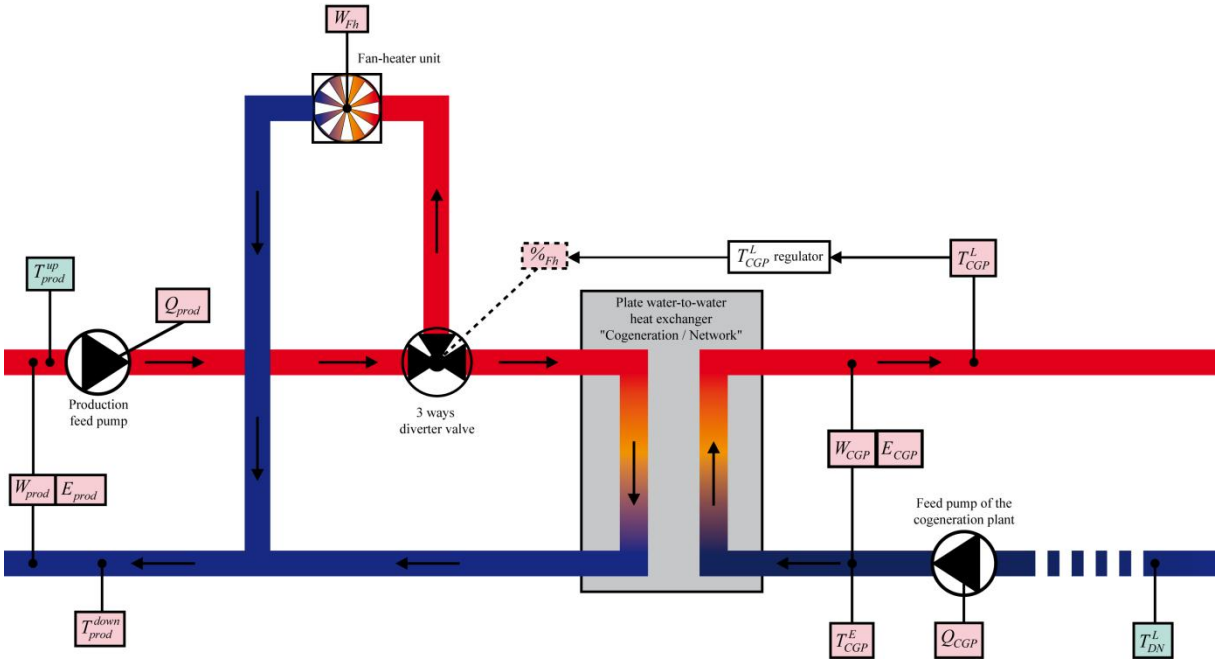

Figure 27. The "cogeneration / network" heat exchanger.

As previously mentioned, a part of the cold water coming back from the distribution network is warmed up by the cogeneration plant, using a plate water-to-water heat exchanger (defined as the "cogeneration/network" exchanger) (Figure 27) which is fed by the hot water passing through the internal circuit of the plant. Let us also note that a part of the water coming from the cogeneration plant get bypassed towards a fan-heater unit to avoid the temperature of the water to be mixed with the water coming back directly from the distribution network to be higher than 73°C. The cogeneration plant has two gas engines of 2.5 MW (Figure 28). The model of the plant has one input (T^{L}_{DN}) and fourteen outputs: Q_{CGP}, T^{E}_{CGP}, W_{CGP}, E_{CGP}, T^{L}_{CGP}, $\%_{fh}$, W_{fh}, T^{up}_{prod}, T^{down}_{prod}, Q_{prod}, W_{prod}, E_{prod}, T^{L}_{PR} and T^{L}_{ECE} (Figure 29).

4.8.1. Flow of the water warmed up by the cogeneration plant

The water entering the breaking pressure bottle is coming back from the distribution network after being partially warmed up by the cogeneration plant (section 4.6.1). Because the flow of the water warmed up by the cogeneration plant (Q_{CGP}) is unchanged when the plant works, one can state that (45):

$$Q_{CGP} = Q_{CGP\_nom} = 120\, m^3.h^{-1} \tag{45}$$

4.8.2. Temperature of the water entering the cogeneration plant

Due to thermal losses in the tubing, the temperature of the water entering the cogeneration plant (T_{CGP}^{E}) and going to the "cogeneration/network" exchanger is not exactly the same as the temperature of the water leaving the distribution network (T_{DN}^{L}) (section 4.7.5). It is slightly lower. Using equation 46, one can estimate T_{CGP}^{E} from T_{DN}^{L}, taking into account the just-mentioned thermal losses, with $\beta^{T_{CGP}^{E}}$ and $\gamma^{T_{CGP}^{E}}$ two parameters to be identified and k the time index:

$$T_{CGP}^{E}(k+1) = \beta^{T_{CGP}^{E}} \cdot T_{DN}^{L} + \gamma^{T_{CGP}^{E}} \tag{46}$$

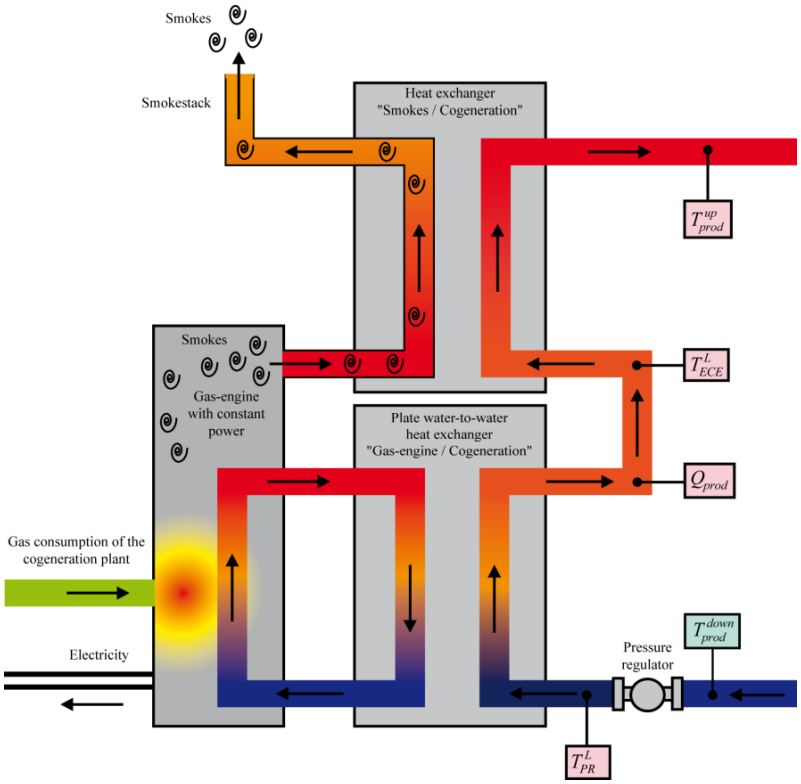

Figure 28. The cogeneration plant.

4.8.3. Production flow

The production flow (Q_{prod}) is the flow of the water passing through the internal circuit of the cogeneration plant. Because this flow is unchanged when the plant works, one can state that (47):

$$Q_{prod} = Q_{prod\_nom} = 108\, m^3 \cdot h^{-1} \tag{47}$$

4.8.4. Fan-heater working

The fan-heater unit allows evacuating a part of the produced heat when the temperature of the water leaving the "cogeneration/network" exchanger is higher than 73°C. The working of the fan-heater unit is related to the opening percentage of its valve ($\%_{fh}$), allowing the unit to be partially fed by the production flow (Q_{prod}). One needs to model $\%_{fh}$ because it impacts on the heat exchange which occurs in the plate heat exchanger. Let us note that the fan-heater power being unchanged when the temperature of the water leaving the plate heat exchanger is lower than 73°C, we considered a minimal opening percentage of the valve equal to 50%. We adjusted this minimal value using a proportional gain (Kp^{fh}) assigned to the difference between the temperature of the water leaving the cogeneration plant (T_{CGP}^{L}) and a temperature of 73°C (48). If $Kp^{fh} \cdot (T_{CGP}^{L}(k) - 73) \leq 0$, then $Kp^{fh} \cdot (T_{CGP}^{L}(k) - 73) = 0$ while if $Kp^{fh} \cdot (T_{CGP}^{L}(k) - 73) \geq 50$, then $Kp^{fh} \cdot (T_{CGP}^{L}(k) - 73) = 50$. As a consequence, $\%_{fh}$ varies between 50 and 100%:

$$\%_{fh}(k+1) = 50 + Kp^{fh} \cdot \left(T_{CGP}^{L}(k) - 73\right) \tag{48}$$

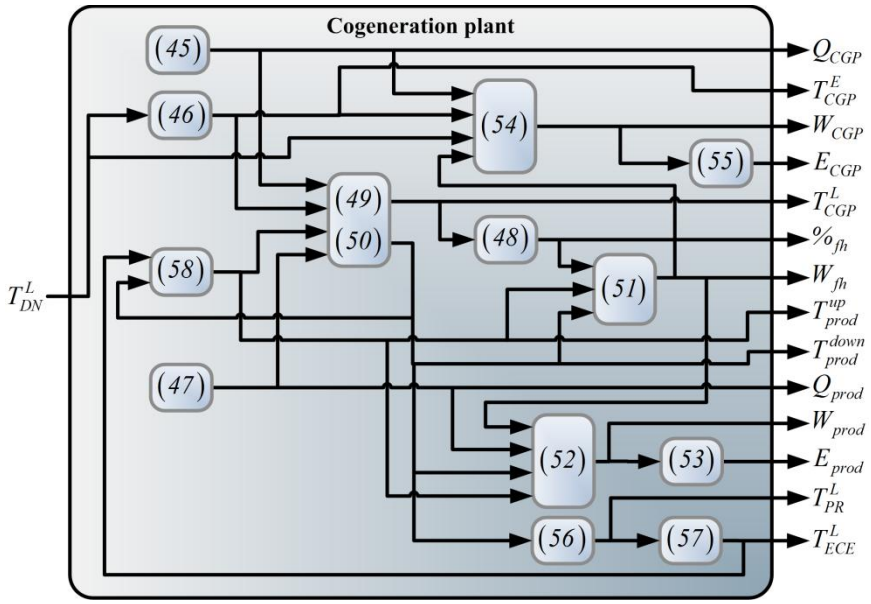

Figure 29. Cogeneration plant model (in brackets, the model equations).

4.8.5. Temperature of the water leaving the cogeneration plant

As previously mentioned, the water leaving the cogeneration plant (after being warmed up) (T_{CGP}^{L}) is mixed with the water coming back directly from the distribution network and enters the breaking pressure bottle. T_{CGP}^{L} can be expressed, using equation 49, with T_{CGP}^{E} the temperature of the water entering the cogeneration plant, T_{prod}^{up} the temperature of the water passing through the internal circuit of the cogeneration plant, before being cooled down by the "cogeneration/network" exchanger, $\alpha^{T_{CGP}^{L}}$, $\beta_1^{T_{CGP}^{L}}$ and $\beta_2^{T_{CGP}^{L}}$ the parameters to be identified and k the time index. The two temperatures are weighted using $Q_{CGP} = Q_{CGP}^{E} = Q_{CGP}^{L}$ and Q_{prod} respectively:

$$T_{CGP}^{L}(k+1) = \alpha^{T_{CGP}^{L}} \cdot T_{CGP}^{L}(k) + \beta_1^{T_{CGP}^{L}} \cdot T_{CGP}^{E}(k) \cdot Q_{CGP}(k) + \beta_2^{T_{CGP}^{L}} \cdot T_{prod}^{up}(k) \cdot Q_{prod}(k) \quad (49)$$

4.8.6. Temperature of the water passing through the internal circuit of the cogeneration plant, after being cooled down by the "cogeneration/network" exchanger

The water passing through the internal circuit of the cogeneration plant, after being cooled down by the "cogeneration/network" exchanger goes back at the heart of the plant to be warmed again. The temperature of this water (T_{prod}^{down}) can be expressed in the same way that T_{CGP}^{L} was (section 4.8.5), with $\alpha^{T_{prod}^{down}}$, $\beta_1^{T_{prod}^{down}}$ and $\beta_2^{T_{prod}^{down}}$ the parameters to be identified and k the time index (50):

$$T_{prod}^{down}(k+1) = \alpha^{T_{prod}^{down}} \cdot T_{prod}^{down}(k) + \beta_1^{T_{prod}^{down}} \cdot T_{CGP}^{E}(k) \cdot Q_{CGP}(k) + \beta_2^{T_{prod}^{down}} \cdot T_{prod}^{up}(k) \cdot Q_{prod}(k) \quad (50)$$

4.8.7. Fan-heater power dissipation

As just mentioned, the fan-heater unit allows evacuating a part of the produced heat when the temperature of the water leaving the "cogeneration/network" exchanger is higher than 73°C. The fan-heater power dissipation (W_{fh}) is expressed using equation (51), with $\%_{fh}$ the opening percentage of its valve, T_{prod}^{up} and T_{prod}^{down} the temperatures of the water passing through the internal circuit of the cogeneration plant, before and after being cooled down by the "cogeneration/network" exchanger respectively, $\beta_1^{W_{fh}}$, $\beta_2^{W_{fh}}$, $\beta_3^{W_{fh}}$ and $\gamma^{W_{fh}}$ the parameters to be identified and k the time index:

$$W_{fh}(k+1) = \beta_1^{W_{fh}} \cdot \left(\%_{fh}(k) + \gamma^{W_{fh}}\right) \cdot \left(\beta_2^{W_{fh}} \cdot T_{prod}^{down}(k) + \beta_3^{W_{fh}} \cdot T_{prod}^{up}(k)\right) \quad (51)$$

4.8.8. Power and energy provided to the "cogeneration/network" exchanger

The power provided to the "cogeneration/network" exhanger and used to warm up a part of the water coming back from the distribution network, called production power (W_{prod}), is calculated

using the production flow (Q_{prod}), the difference between the temperatures of the water passing through the internal circuit of the cogeneration plant, before (T_{prod}^{up}) and after (T_{prod}^{down}) being cooled down by the just-mentioned exchanger, as well as the fan-heater power dissipation (W_{fh}). Let us note that the impact of W_{fh} on W_{prod} is not well understood (52). One can also calculate the energy (E_{prod}) related to W_{prod} (53). $\rho_{water} = 971.6\, kg.m^{-3}$ and $Cp_{water} = 4196\, J.kg^{-1}.K^{-1}$ are the density and the specific heat capacity of water respectively, k is time index, T_E is the sampling time and $\beta^{W_{prod}}$ and $\gamma^{W_{prod}}$ are two parameters to be identified:

$$W_{prod}(k+1) = \frac{Q_{prod}(k) \cdot \left(T_{prod}^{up}(k) - T_{prod}^{down}(k)\right) \cdot \rho_{water} \cdot Cp_{water}}{3600} - \beta^{W_{prod}} \cdot W_{fh}(k) + \gamma^{W_{prod}} \quad (52)$$

$$E_{prod}(k+1) = E_{prod}(k) + \frac{W_{prod}(k) \cdot T_E}{3600 \times 1000} \quad (53)$$

4.8.9. Power and energy provided by the cogeneration plant

As a result of the thermal exchange one can observe with the cogeneration plant, both the power (W_{CGP}) and the energy (E_{CGP}) absorbed by the water to be warmed up and passing through the distribution network can be expressed, using equations (54) and (55) respectively, in the same way we expressed the power and the energy provided to the "cogeneration/network" exchanger (section 4.8.8) but with Q_{CGP} the flow of the water warmed up by the cogeneration plant, T_{CGP}^{E} and T_{CGP}^{L} the temperatures of the water entering and leaving the plant respectively, $\beta^{W_{CGP}}$ and $\gamma^{W_{CGP}}$ two parameters to be identified and k the time index:

$$W_{CGP}(k+1) = \frac{Q_{CGP}(k) \cdot \left(T_{CGP}^{L}(k) - T_{CGP}^{E}(k)\right) \cdot \rho_{water} \cdot Cp_{water}}{3600} - \beta^{W_{CGP}} \cdot W_{fh}(k) + \gamma^{W_{CGP}} \quad (54)$$

$$E_{CGP}(k+1) = E_{CGP}(k) + \frac{W_{CGP}(k) \cdot T_E}{3600 \times 1000} \quad (55)$$

4.8.10. Temperature of the water cooled down by the pressure regulator

First, the cold water coming back from distribution network is cooled down and its pressure is reduced by a pressure regulator. Let us note that the water leaving this regulator is the coolest inside the cogeneration plant. Its temperature (T_{PR}^{L}) is fully correlated to the temperature of the water passing through the internal circuit of the cogeneration plant, after being cooled down by the "cogeneration/network" exchanger (T_{prod}^{down}) (section 4.8.6), and can be expressed as follows, with $\alpha^{T_{PR}^{L}}$, $\beta^{T_{PR}^{L}}$ and $\gamma^{T_{PR}^{L}}$ three parameters to be identified and k the time index (56):

$$T_{PR}^{L}(k+1) = \alpha^{T_{PR}^{L}} \cdot T_{PR}^{L}(k) + \beta^{T_{PR}^{L}} \cdot T_{prod}^{down}(k) + \gamma^{T_{PR}^{L}} \quad (56)$$

4.8.11. Temperature of the water warmed up by the "engine/cogeneration" exchanger

The water leaving the pressure regulator is then warmed up by a plate water-to-water heat exchanger, named "engine/cogeneration" exchanger, while passing trough an internal water circuit and using calories provided by the gas engine burner. Because its power remains unchanged, the temperature of the water warmed up by the just-mentioned exchanger (T_{ECE}^{L}) is linearly dependend on the temperature of the water cooled down by the pressure regulator (T_{PR}^{L}). As a consequence, T_{ECE}^{L} can be expressed, using equation (57), with $\alpha^{T_{ECE}^{L}}$, $\beta^{T_{ECE}^{L}}$ and $\gamma^{T_{ECE}^{L}}$ three parameters to be identified and k the time index:

$$T_{ECE}^{L}(k+1) = \alpha^{T_{ECE}^{L}} \cdot T_{ECE}^{L}(k) + \beta^{T_{ECE}^{L}} \cdot T_{PR}^{L}(k) + \gamma^{T_{ECE}^{L}} \quad (57)$$

4.8.12. Temperature of the water passing through the internal circuit of the cogeneration plant, before being cooled down by the "cogeneration/network" exchanger

The hot water leaving the "engine/cogeneration" exchanger is warmed up again while passing through another heat exchanger (named "smoke/cogeneration" exchanger), using hot smokes

whose temperature is about 230°C, as a result of gas combustion. Next, this water will enter the "cogeneration/network" exchanger to be cooled down. Its temperature (T_{prod}^{up}) can be expressed, using equation (58), with T_{ECE}^{L} the temperature of the water warmed up by the "engine/cogeneration" exchanger, T_{prod}^{down} the temperature of the water passing through the internal circuit of the cogeneration plant, after being cooled down by the "cogeneration/network" exchanger, $\alpha^{T_{prod}^{up}}$, $\beta_1^{T_{prod}^{up}}$, $\beta_2^{T_{prod}^{up}}$ et $\gamma^{T_{prod}^{up}}$ four parameters to be identified and k the time index:

$$T_{prod}^{up}(k+1) = \alpha^{T_{prod}^{up}} \cdot T_{prod}^{up}(k) + \beta_1^{T_{prod}^{up}} \cdot T_{ECE}^{L}(k) + \beta_2^{T_{prod}^{up}} \cdot T_{prod}^{down}(k) + \gamma^{T_{prod}^{up}} \quad (58)$$

4.8.13. Identification results

Table 11 (Appendix) deals with the identification process of the parameters of the cogeneration plant model. Over-all, the model accuracy can be considered as satisfactory. Let us highlight that the respective temperatures of the water entering (T_{CGP}^{E}) (Figure 30) and leaving (T_{CGP}^{L}) (Figure 31) the cogeneration plant are well modelled for the considered period. As previously mentioned, T_{CGP}^{L} is of paramount interest because it is related to the water which is mixed with the water coming back directly from the distribution network and enters the breaking pressure bottle. As a consequence, its good estimation is mandatory for correctly simulating the behaviour of the district boiler of La Rochelle. Both the FIT and the MRE are about 64% and 1% for T_{CGP}^{E} and about 33% and 3% for T_{CGP}^{L}. One can also highlight that due to the lack of information (for example about the fan-heater unit), the temperatures of the water passing through the internal circuit of the cogeneration plant are not so well modelled. For the same reasons, the power calculations are dubious.

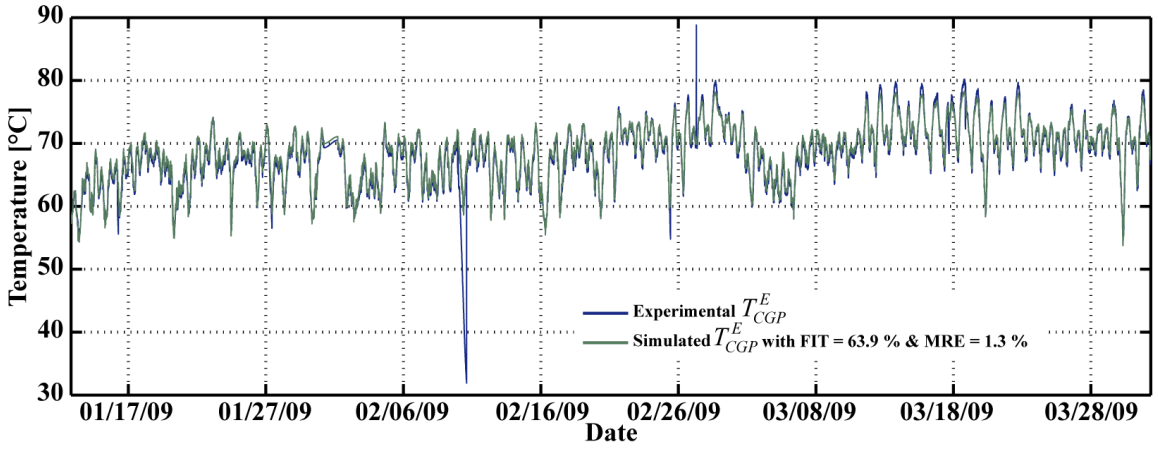

Figure 30. Temperature of the water entering the cogeneration plant.

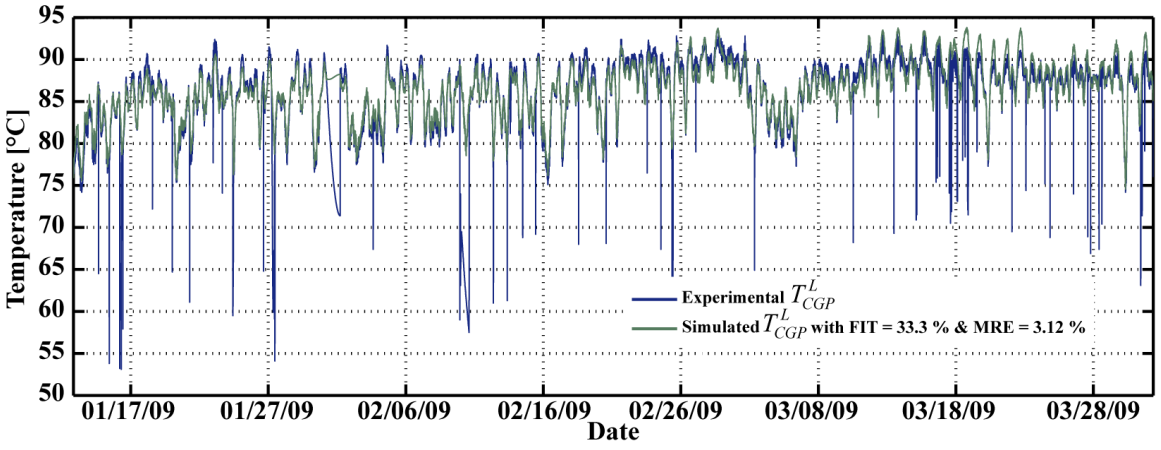

Figure 31. Temperature of the water leaving the cogeneration plant.

4.9. District boiler

As it was previously mentioned, the aim of the present work was to model the district boiler of La Rochelle. That is why all the sub-systems models, presented in sections 4.2 to 4.8, were brought together to obtain the global model of the boiler whose inputs are two exogenous parameters: the outdoor temperature and the thermal power consumption of the hot water distribution network. First, this global model will be used to simulate the district boiler behaviour on the long range (a few months), for example during a complete heating period. As a consequence, the proposed model has to remain stable on the long range and will be used to optimize the district boiler performance while adding to the plant a thermal storage unit or modifying some parameters related to regulations (for example, temperature set-points). Next, this global model can be used to simulate the district boiler behaviour on the short range (a few hours) to optimize its functioning in real-time. Such a simulation will be useful to both implement and tune a Model Predictive Controller (MPC) by solving online an optimization problem where the decision variables provide the control action. Finally, let us remember that the OptiEnR research project deals with the reduction of the coverage rate of the fossil energy boiler. To check both the validity and the accuracy of the developed global model, in the two ways it can be used, we calculated the Mean Relative Error (MRE) between experimental and estimated values. Tables 12 to 18 (Appendix) present, first, the MRE obtained for each sub-system model during its identification phase and, secondly, the MRE obtained when considering the global model and simulating on the long or the short range (again for each sub-system model). Tables 12 to 18 (Appendix) only deal with parameters we can compare estimated and experimental data. As a consequence, theses tables do not make mention of the flow of the distribution network (Q_{DN}) or the real-time ($Fuel_{rt}$), daily ($Fuel_d$) and cumulative ($Fuel_c$) consumptions of fuel oil. The results show that the proposed global model is able to describe correctly the behaviour of the district boiler of La Rochelle even if, at times, some parameters are not well estimated. One can highlight first that the estimation of the cumulative consumption of gas (Gas_c) is very accurate while the wood consumption is slightly underestimated, in particular at the end of the considered period (From early January to late March 2009). One can also note that, for some parameters (mainly T_{SC}, T_{SGFB}, T_{WB}^L, Q_{CHC}^L, T_{CHC}^E, T_{BPB}^L and W_{CGP}), bringing together all the sub-systems models leads to an increase of the mean relative error when simulating on the long or the short range.

5. Conclusion

As part of the OptiEnR research project, the present paper focuses on both the analysis and the modelling of the district boiler of La Rochelle (east cost of France). This district boiler is composed of two thermal boilers and supplies hot water via a distribution network. The first boiler, a wood boiler, uses renewable energy while the second one, a gas-fuel oil boiler, uses fossil energy. The final objective of the project deals with improving the performance of the plant, using a model-based predictive controller to manage a to-be-implemented thermal storage unit. One wants to minimize the use of fossil energy, stocking renewable energy during low-demand periods and using it when demand is high. Due to the complexity of the district boiler of La Rochelle as a whole, as well as the strong interactions between sub-systems (i.e. the wood boiler, the gas-fuel oil boiler, the breaking pressure bottle, the collecting hydraulic circuit, the cogeneration plant and the distribution network), we proposed a modular approach for modelling the plant. According to what information is available (thanks to measurement campaigns or taking into consideration the expert knowledge about the sub-systems functioning and the boilers control systems), a combination of white, grey and black boxes has been used. Let us note that, due to the lack of information about the wood boiler functioning (the main component of the district boiler of La Rochelle) and in particular related to wood consumption (whose influence on the model performance is significant), we used a black box Hammerstein-Wiener model, composed of a linear and two nonlinear blocks. One can also highlight that, because of both the lack of information and a low sampling time (5 minutes), planning the way the gas-fuel oil boiler is engaged is relatively complex. Moreover, and because no measurements are carried out at the district boiler, the consumption of fuel oil has been modelled with difficulties, using an energy ratio between gas and fuel oil. However, and whatever the sub-system we consider, the correlation between the real and estimated parameters is pretty high (notably when taking a look at the most significant parameters, such as the consumptions of gas and fuel oil or both the flow and the temperature of the water passing through the collecting

hydraulic circuit and the distribution network). The results show that the proposed global model, even if bringing together all the sub-systems models leads to a deterioration of their performance, is able to describe correctly the behaviour of the district boiler of La Rochelle. When simulating on the short (a few hours) or the long (a few months) range, while considering the influence of both the outdoor temperature and the thermal power consumption of the hot water distribution network, this deterioration stills under control. As key points, one can note, first, that the estimated cumulative consumptions of wood ($Wood_c$) and gas (Gas_c) are very accurate and, secondly, that the way the gas-fuel oil boiler is used is well modelled.

Future work will now focus on, first, studying the feasibility of integrating to the plant a thermal storage unit and choosing the most adequate storage material, secondly, on modelling the thermal storage unit we want to implement and, finally, on optimizing the district boiler functioning using a model predictive controller and forecasted sequences about the outdoor temperature and the thermal power consumed by the hot water distribution network.

Appendix: identification results

Table 1. Global regulation of the district boiler.

Parameter	*Value*	*Unit*	*Parameter*	*Value*	*Unit*
$T_{out\_SDN_1}$	*-6.096*	*°C*	$T_{out\_SWB_1}$	*-2.368*	*°C*
$T_{out\_SDN_2}$	*3.525*	*°C*	$T_{out\_SWB_2}$	*2.297*	*°C*
$T_{out\_SDN_3}$	*9.615*	*°C*	$T_{out\_SWB_3}$	*10.40*	*°C*
$T_{out\_SND_4}$	*11.19*	*°C*	$T_{out\_SWB_4}$	*16.65*	*°C*
$T_{out\_SDN_5}$	*18.38*	*°C*	T_{SWB_1}	*101.60*	*°C*
T_{SDN_1}	*96.80*	*°C*	T_{SWB_2}	*100.40*	*°C*
T_{SDN_2}	*84.96*	*°C*	T_{SWB_3}	*87.15*	*°C*
T_{SDN_3}	*82.31*	*°C*	T_{SWB_4}	*85.05*	*°C*
T_{SDN_4}	*80.21*	*°C*	$\alpha^{T_{SGFB}}$	*1.073×10-1*	*-*
T_{SDN_5}	*70.30*	*°C*	$\beta^{T_{SGFB}}$	*8.783×10-1*	*-*

Table 2. Input nonlinear block (T_{WB}^E).

Parameter	*Value (°C)*	*Parameter*	*Value*	*Parameter*	*Value (°C)*	*Parameter*	*Value*
$x_1^{T_{WB}^E}$	*70.27*	$y_1^{T_{WB}^E}$	*3.324×10²*	$x_6^{T_{WB}^E}$	*84.71*	$y_6^{T_{WB}^E}$	*1.604×10²*
$x_2^{T_{WB}^E}$	*73.91*	$y_2^{T_{WB}^E}$	*7.732×10²*	$x_7^{T_{WB}^E}$	*88.06*	$y_7^{T_{WB}^E}$	*1.270×10²*
$x_3^{T_{WB}^E}$	*75.62*	$y_3^{T_{WB}^E}$	*8.951×10²*	$x_8^{T_{WB}^E}$	*92.13*	$y_8^{T_{WB}^E}$	*8.702×10²*
$x_4^{T_{WB}^E}$	*78.64*	$y_4^{T_{WB}^E}$	*1.118×10²*	$x_9^{T_{WB}^E}$	*95.17*	$y_9^{T_{WB}^E}$	*5.097×10²*
$x_5^{T_{WB}^E}$	*82.68*	$y_5^{T_{WB}^E}$	*1.494×10²*	$x_{10}^{T_{WB}^E}$	*98.62*	$y_{10}^{T_{WB}^E}$	*1.561×10²*

Table 3. Input nonlinear block (T_{SWB}).

Parameter	*Value (°C)*	*Parameter*	*Value*	*Parameter*	*Value (°C)*	*Parameter*	*Value*
$x_1^{T_{SWB}}$	*68.58*	$y_1^{T_{SWB}}$	*-3.365×10¹*	$x_6^{T_{SWB}}$	*78.26*	$y_6^{T_{SWB}}$	*9.756×10¹*
$x_2^{T_{SWB}}$	*69.21*	$y_2^{T_{SWB}}$	*-0.722×10¹*	$x_7^{T_{SWB}}$	*79.59*	$y_7^{T_{SWB}}$	*1.145×10²*
$x_3^{T_{SWB}}$	*70.29*	$y_3^{T_{SWB}}$	*-3.475×10¹*	$x_8^{T_{SWB}}$	*82.58*	$y_8^{T_{SWB}}$	*1.303×10²*
$x_4^{T_{SWB}}$	*71.45*	$y_4^{T_{SWB}}$	*-4.195×10¹*	$x_9^{T_{SWB}}$	*85.42*	$y_9^{T_{SWB}}$	*1.440×10²*
$x_5^{T_{SWB}}$	*75.74*	$y_5^{T_{SWB}}$	*1.172×10¹*	$x_{10}^{T_{SWB}}$	*85.67*	$y_{10}^{T_{SWB}}$	*1.554×10²*

Table 4. Linear block (x_1).

Parameter	*Value*	*Parameter*	*Value*	*Parameter*	*Value*
$\alpha_{11,1}$	*-1.889×10-1*	$\alpha_{11,6}$	*-5.175×10-1*	α_{12}	*8.147×10-1*
$\alpha_{11,2}$	*-4.535×10-2*	$\beta_{11,1}$	*0.100×10¹*	β_{12}	*0.1000×10¹*
$\alpha_{11,3}$	*-9.695×10-2*	$\beta_{11,2}$	*0.1955×10¹*	α_{13}	*-6.470×10-1*
$\alpha_{11,4}$	*-2.006×10-1*	$\beta_{11,3}$	*-0.5966×10¹*	β_{13}	*0.1000×10¹*
$\alpha_{11,5}$	*3.161×10-1*	$\beta_{11,4}$	*0.3034×10¹*	*-*	*-*

Table 5. Linear block (x_2).

Parameter	*Value*	*Parameter*	*Value*	*Parameter*	*Value*
α_{11}	*-9.536×10⁻¹*	$\alpha_{12,2}$	*-4.344×10⁻¹*	$\alpha_{13,2}$	
$\beta_{11,1}$	*-3.913×10⁻¹*	$\alpha_{12,3}$	*-5.121×10⁻¹*	$\alpha_{13,3}$	*-1.747×10⁻¹*
$\beta_{11,2}$	*0.1000×10¹*	$\alpha_{12,4}$	*-4.894×10⁻¹*	$\alpha_{13,4}$	*2.418×10⁻²*
$\beta_{11,3}$	*-8.490×10⁻¹*	$\alpha_{12,5}$	*9.400×10⁻¹*	$\alpha_{13,5}$	*4.878×10⁻²*
$\beta_{11,4}$	*2.396×10⁻¹*	β_{12}	*2.079×10⁻³*	β_{13}	*8.769×10⁻²*
$\alpha_{12,1}$	*-4.976×10⁻¹*	$\alpha_{13,1}$	*4.672×10⁻¹*	-	-

Table 6. Output nonlinear block (N_{tappet}).

Parameter	*Value*	*Parameter*	*Value*	*Parameter*	*Value*	*Parameter*	*Value*
$x_1^{N_{tappet}}$	*-3.683×10¹*	$y_1^{N_{tappet}}$	*10.75*	$x_6^{N_{tappet}}$	*1.317×10²*	$y_6^{N_{tappet}}$	*2.429*
$x_2^{N_{tappet}}$	*0.389×10¹*	$y_2^{N_{tappet}}$	*12.31*	$x_7^{N_{tappet}}$	*1.763×10²*	$y_7^{N_{tappet}}$	*2.393*
$x_3^{N_{tappet}}$	*4.462×10¹*	$y_3^{N_{tappet}}$	*1.667*	$x_8^{N_{tappet}}$	*2.111×10²*	$y_8^{N_{tappet}}$	*2.481*
$x_4^{N_{tappet}}$	*7.103×10¹*	$y_4^{N_{tappet}}$	*3.111*	$x_9^{N_{tappet}}$	*2.956×10²*	$y_9^{N_{tappet}}$	*2.373*
$x_5^{N_{tappet}}$	*1.023×10²*	$y_5^{N_{tappet}}$	*2.776*	$x_{10}^{N_{tappet}}$	*5.107×10²*	$y_{10}^{N_{tappet}}$	*2.508*

Table 7. Output nonlinear block (T_{WB}^L).

Parameter	*Value*	*Parameter*	*Value (°C)*	*Parameter*	*Value*	*Parameter*	*Value (°C)*
$x_1^{T_{WB}^L}$	*-3.106×10¹*	$y_1^{T_{WB}^L}$	*67.80*	$x_6^{T_{WB}^L}$	*-1.004×10¹*	$y_6^{T_{WB}^L}$	*81.61*
$x_2^{T_{WB}^L}$	*-2.507×10¹*	$y_2^{T_{WB}^L}$	*75.16*	$x_7^{T_{WB}^L}$	*5.056×10¹*	$y_7^{T_{WB}^L}$	*95.19*
$x_3^{T_{WB}^L}$	*-2.101×10¹*	$y_3^{T_{WB}^L}$	*76.41*	$x_8^{T_{WB}^L}$	*6.471×10¹*	$y_8^{T_{WB}^L}$	*76.95*
$x_4^{T_{WB}^L}$	*-1.517×10¹*	$y_4^{T_{WB}^L}$	*43.16*	$x_9^{T_{WB}^L}$	*1.021×10²*	$y_9^{T_{WB}^L}$	*93.79*
$x_5^{T_{WB}^L}$	*-1.509×10¹*	$y_5^{T_{WB}^L}$	*43.47*	$x_{10}^{T_{WB}^L}$	*1.054×10²*	$y_{10}^{T_{WB}^L}$	*88.28*

Table 8. Gas-fuel oil boiler.

Parameter	*Value*	*Parameter*	*Value*	*Parameter*	*Value*	*Parameter*	*Value*
α^{gas}	*4.750×10⁻¹*	β_2^{smo}	*8.813×10⁻¹*	$\beta_1^{T_{GFB}^L}$	*-7.570×10⁻²*	$\beta_5^{T_{GFB}^L}$	*7.228×10⁻¹*
β^{gas}	*0.2981×10¹*	β_3^{smo}	*7.125×10⁻¹*	$\beta_2^{T_{GFB}^L}$	*1.748×10¹*	$\beta_6^{T_{GFB}^L}$	*-0.3516×10¹*
γ^{gas}	*-6.307×10¹*	γ^{smo}	*0.4168×10¹*	$\beta_3^{T_{GFB}^L}$	*3.978×10⁻¹*	$\beta_7^{T_{GFB}^L}$	*1.063×10⁻¹*
α^{smo}	*6.884×10⁻¹*	$\alpha_1^{T_{GFB}^L}$	*7.362×10⁻¹*	$\beta_4^{T_{GFB}^L}$	*2.113×10⁻²*	$\gamma^{T_{GFB}^L}$	*1.924×10⁻¹*
β_1^{smo}	*2.286×10⁻¹*	$\alpha_2^{T_{GFB}^L}$	*6.083×10⁻¹*	-	-	-	-

Table 9. Collecting hydraulic circuit.

Parameter	*Value*	*Parameter*	*Value*
$\alpha_1^{T_{GFB}^E}$	*6.291×10⁻¹*	$\beta_1^{T_{GFB}^E}$	*3.769×10⁻¹*
$\alpha_2^{T_{GFB}^E}$	*-2.353×10⁻¹*	$\delta_1^{T_{GFB}^E}$	*0.5680×10¹*
$\alpha_3^{T_{GFB}^E}$	*-1.142×10⁻³*	$\alpha_1^{T_{WB}^E}$	*2.759×10⁻¹*
$\alpha_4^{T_{GFB}^E}$	*-1.214×10⁻¹*	$\alpha_2^{T_{WB}^E}$	*7.321×10⁻¹*
$\alpha_5^{T_{GFB}^E}$	*0.7744×10¹*	$\beta_1^{T_{WB}^E}$	*9.996×10⁻¹*
$\alpha_6^{T_{GFB}^E}$	*-9.977×10⁻¹*	-	-

Table 10. Hot water distribution network.

Parameter	Value	Parameter	Value	Parameter	Value
α^{fp}	-2.702×10^{-1}	β_3^{fp}	1.913×10^{1}	$\gamma^{Q_{DN}^E}$	0.2017×10^{1}
β_1^{fp}	4.514×10^{1}	γ^{fp}	1.203×10^{1}	$\eta^{Q_{DN}^E}$	0.1852×10^{1}
β_2^{fp}	-0.1552×10^{1}	$\beta^{Q_{DN}^E}$	1.461×10^{-2}	$\kappa^{Q_{DN}^E}$	$-478\ m^3.h^{-1}$

Table 11. Cogeneration plant.

Parameter	Value	Parameter	Value	Parameter	Value
$\beta^{T_{CGP}^E}$	0.1025×10^{1}	$\beta_1^{W_{fh}}$	4.317×10^{-1}	$\beta^{T_{PR}^L}$	2.346×10^{-2}
$\gamma^{T_{CGP}^E}$	-0.3362×10^{1}	$\beta_2^{W_{fh}}$	0.2073×10^{1}	$\gamma^{T_{PR}^L}$	-0.1276×10^{1}
Kp^{fh}	1.375×10^{1}	$\beta_3^{W_{fh}}$	-0.1401×10^{1}	$\alpha^{T_{ECE}^L}$	0
$\alpha^{T_{CGP}^L}$	-5.942×10^{-1}	$\gamma^{W_{fh}}$	3.022×10^{1}	$\beta^{T_{ECE}^L}$	2.231×10^{-1}
$\beta_1^{T_{CGP}^L}$	9.810×10^{-3}	$\beta^{W_{prod}}$	0.4416×10^{1}	$\gamma^{T_{ECE}^L}$	7.774×10^{1}
$\beta_2^{T_{CGP}^L}$	5.738×10^{-3}	$\gamma^{W_{prod}}$	2.361×10^{2}	$\alpha^{T_{prod}^{up}}$	-3.174×10^{-1}
$\alpha^{T_{prod}^{down}}$	9.636×10^{-1}	$\beta^{W_{CGP}}$	1.092×10^{1}	$\beta_1^{T_{prod}^{up}}$	-0.1242×10^{1}
$\beta_1^{T_{prod}^{down}}$	9.471×10^{-5}	$\gamma^{W_{CGP}}$	5.844×10^{2}	$\beta_2^{T_{prod}^{up}}$	7.276×10^{-1}
$\beta_2^{T_{prod}^{down}}$	1.743×10^{-4}	$\alpha^{T_{PR}^L}$	9.930×10^{-1}	$\gamma^{T_{prod}^{up}}$	3.447×10^{-1}

Table 12. Global regulation of the district boiler (global model of the district boiler).

Parameter	MRE (identification)	MRE (long range)	MRE (short range)
T_{SDN}	2.87%	2.45%	2.42%
T_{SWB}	7.31%	5.6%	5.44%
T_{SC}	7.76%	21.9%	16.7%
T_{SGFB}	8.05%	21.7%	16.4%

Table 13. Wood boiler (global model of the district boiler).

Parameter	MRE (identification)	MRE (long range)	MRE (short range)
N_{tappet}	16.6%	20.9%	21.3%
T_{WB}^L	7.28%	16.1%	15.3%
$Wood_d$	4.28%	4.33%	4.28%
$Wood_c$	0.825%	2.64%	3.59%

Table 14. Gas-fuel oil boiler (global model of the district boiler).

Parameter	MRE (identification)	MRE (long range)	MRE (short range)
Gas_{rt}	2.34%	7.6%	6.19%
Gas_d	3.02%	8.27%	1.48%
Gas_c	0.589%	1.83%	0.133%
T_{GFB}^{smo}	4.13%	10.8%	7.79%
T_{GFB}^L	9.47%	16.2%	13.7%

Table 15. Collecting hydraulic circuit (global model of the district boiler).

Parameter	MRE (identification)	MRE (long range)	MRE (short range)
T_{CHC}^E	3.82%	15.2%	5.07%
Q_{CHC}^L	0.5%	24%	17.9%
T_{GFB}^E	1.6%	17.8%	15.6%
T_{WB}^E	1.77%	14%	13.2%

Table 16. Breaking pressure bottle (global model of the district boiler).

Parameter	*MRE (identification)*	*MRE (long range)*	*MRE (short range)*
T_{CHC}^{E}	*3.54%*	*19.4%*	*17.6%*
T_{BPB}^{L}	*2.81%*	*15.6%*	*14.6%*

Table 17. Hot water distribution network (global model of the district boiler).

Parameter	*MRE (identification)*	*MRE (long range)*	*MRE (short range)*
P_{SDN}	*0.674%*	*0.58%*	*0.574%*
P_{DN}	*5.01%*	*5.03%*	*5.02%*
$\%_{fp}$	*4.3%*	*4.43%*	*4.42%*
T_{DN}^{L}	*0%*	*16.4%*	*17.6%*

Table 18. Cogeneration plant (global model of the district boiler).

Parameter	*MRE (identification)*	*MRE (long range)*	*MRE (short range)*
Q_{CGP}	*2.9%*	*3.41%*	*3.36%*
T_{CGP}^{E}	*1.3%*	*8.76%*	*7.94%*
Q_{prod}	*1.95%*	*2.41%*	*2.37%*
T_{CGP}^{L}	*3.12%*	*14.7%*	*13.9%*
T_{prod}^{down}	*3.79%*	*5.43%*	*3.39%*
W_{fh}	*6.06%*	*6.95%*	*110.1%*
W_{prod}	*5.42%*	*3.9%*	*5.7%*
W_{CGP}	*5.99%*	*25.1%*	*24.9%*
T_{PR}^{L}	*6.43%*	*10.2%*	*5.7%*
T_{ECE}^{L}	*1.86%*	*3.16%*	*2.38%*
T_{prod}^{up}	*7.67%*	*8.34%*	*7.72%*

References

[1] A. Caillé, M. Al-Moneef, F. Barnés de Castro, A. Bundgaard-Jensen, A. Fall, N. Franco de Medeiros, C.P. Jain, Y.D. Kim, M.J. Nadeau, C. Testa, J. Teyssen, E. Velasco Garcia, R. Wood, Z. Guobao, G. Doucet, 2007 survey of energy resources, Technical Report, World Energy Council, 2007.

[2] Europe's energy position. Present & future, Market Observatory for Energy, 2008.

[3] J. Eynard, S. Grieu, M. Polit, Wavelet-based multi-resolution analysis and artificial neural networks for forecasting temperature and thermal power consumption, Engineering Applications of Artificial Intelligence (2010), doi: 10.1016/j.engappai.2010.09.003.

[4] Cofely GDF-SUEZ, http://www.cofely-gdfsuez.fr/en/homepage/.

[5] Weiss France, http://www.weiss-france.fr/index.php?_lngweb=en.

[6] C.E. Garcia, D.M. Prett, Model predictive control: Theory and practive. A survey, Automatica 25 (3) (1989) 335-348.

[7] S.J. Qin, T.A. Badgwell, A survey of industrial model predictive control technology, Control Engineering Practice 11 (2003) 733-764.

[8] V. Curti, M.R. von Spakovsky, D. Favrat, An environomic approach for the modeling and optimization of a district heating network based on centralized and decentralized heat pumps, cogeneration and/or gas furnace. Part I: Methodology, International Journal of Thermal Sciences 39 (2000) 721-730.

[9] R. Dias, J. Balestieri, Energetic and exergetic analysis in a firewood boiler, Revista de Ciencia & Tecnologia 12 (2004) 15-24.

[10] J. Gonzalez-Bustamante, J. Sala, L. Lopez-Gonzalez, J.L. Miguez, I. Flores, Modelling and dynamic simulation of processes with MATLAB. An application of a natural gas installation in a power plant, Energy 32 (2007) 1271-1282.

[11] Z. Niu, K.F.V. Wong, Adaptive simulation of boiler unit performance, Energy Conversion and Management 39 (1998) 1383-1394.

[12] S. Prasad, Biomass-fired steam power cogeneration system: a theoretical study, Energy Conversion and Management 36 (1) (1995) 65-77.

[13] T.M.I. Mahlia, M.Z. Abdulmuin, T.M.I. Alamsyah, D. Mukhlishien, Dynamic modelling and simulation of a palm wastes boiler, Renewable energy 28 (2003) 1235-1256.

[14] B.O. Bouamama, K. Medjaher, A. Samantaray, M. Staroswiecki, Supervision of an industrial steam generator. Part I: Bond graph modelling, Control Engineering Practice 14 (2006) 71-83.

[15] S. Lu, B.W. Hogg, Dynamic nonlinear modelling of power plant by physical principles and neural networks, International Journal of Electrical Power & Energy Systems 22 (2000) 67-78.

[16] L.M. Romeo, R. Gareta, Neural network for evaluating boiler behaviour, Applied Thermal Engineering 26 (2006) 1530-1536.

[17] A. Ghaffari, A. Chaibakhsh, C. Lucas, Soft computing approach for modelling power plant with a once-though boiler, Engineering Applications of Artificial Intelligence 20 (2007) 809-819.

[18] J. Sjberg, Q. Zhang, L. Ljung, A. Benveniste, B. Delyon, P.Y. Glorennec, H. Hjalmarsson, A. Juditsky, Nonlinear black-box modelling in system identification: a unified overview, Automatica 31 (1995) 1691-1724.

[19] L. Ljung, System identification: theory for the user, Prentice Hall, 1987.

[20] T. Hsia, System identification: Least-squares methods, Lexington, Mass., D.C. Heath and Co., 1977.

[21] D.M. Tanton, R.R. Cohen, S.D. Probert, Improving the effectiveness of a domestic central-heating boiler by the use of heat storage, Applied Energy 27 (1987) 53-82.

[22] U. Stritih, V. Butala, Optimization of a thermal storage unit combined with a biomass boiler for heating buildings, Renewable Energy 29 (2004) 2011-2022.

[23] M. Cao, J. Cao, Optimal design of thermal-energy stores for boiler plants, Applied Energy 83 (2006) 55-68.

[24] R.H. Byrd, R.B. Schnabel, G.A. Schultz, A trust region algorithm for nonlinearly constrained optimization, SIAM Journal on Numerical Analysis 24 (5) (1987) 1152-1170.

[25] T.F. Coleman, Y. Li, On the convergence of interior-reflective Newton methods for nonlinear minimization subject to bounds, Mathematical Programming 67 (1) (1994) 189-224.

[26] T.F. Coleman, Y. Li, An interior trust region approach for nonlinear minimization subject to bounds, SIAM Journal on Optimization 6 (2) (1996) 418-445.

[27] S. Grieu, V.G. Tran, M. Polit, Q.T. Tran, Transformée en ondelettes discrète et réseaux de neurones artificiels pour la prédiction d'irradiation solaire à court terme, Energies renouvelables et éco-conception en génie électrique, Revue de l'Electricité et de l'Electronique 5 (2009) 52-60.

[28] V.G. Tran, S. Grieu, M. Polit, Q.T. Tran, Forecasting of solar irradiation using wavelets decomposition and cascade-correlation neural networks, International Conference on Renewable Energy and Eco-Design in Electrical Engineering iREED 2008, Montpellier, France, 2008.

[29] V.G. Tran, S. Grieu, M. Polit, Q.T. Tran, H.L. Tran, Forecasting of wind speed using wavelets analysis and cascade-correlation networks, European Wind Energy Conference EWEC 2009, Marseille, France, 2009.

[30] F. Chang, R. Luus, A noniterative method for identification using Hammerstein model, IEEE Transactions on Automatic Control 16 (5) (1971) 464-468.

[31] P. Stoica, T. Söderstrom, Instrumental-variable methods for identification of Hammerstein systems, International Journal of Control 35 (3) (1982) 459-476.

[32] Y. Zhu, Identification of Hammerstein models for control using ASYM, International Journal of Control 73 (18) (2000) 1692-1702.

[33] W. Greblicki, Nonparametric identification of Wiener systems, IEEE Transactions on Information Theory 38 (5) (1992) 1487-1493.

[34] T. Wigren, Recursive prediction error identification using the nonlinear Wiener model, Automatica 29 (4) (1993) 1011-1025.

[35] Y. Zhu, Parametric Wiener model identification for control, 14th World Congress of IFAC, Beijing, China, 1999.

[36] Y. Zhu, Estimation of an N-L-N Hammerstein-Wiener model, Automatica 38 (9) (2002) 1607-1614.